

Asymptotic behavior of large polygonal Wilson loops in confining gauge theories

P.V. Pobylitsa

*Petersburg Nuclear Physics Institute
Gatchina, 188300, St. Petersburg, Russia*

Abstract

In the framework of effective string theory (EST), the asymptotic behavior of a large Wilson loop in confining gauge theories can be expressed via Laplace determinant with Dirichlet boundary condition on the Wilson contour. For a general polygonal region, Laplace determinant can be computed using the conformal anomaly and Schwarz-Christoffel transformation. One can construct ratios of polygonal Wilson loops whose large-size limit can be expressed via computable Laplace determinants and is independent of the (confining) gauge group. These ratios are computed for hexagon polygons both in EST and by Monte Carlo (MC) lattice simulations for the tree-dimensional lattice \mathbb{Z}_2 gauge theory (dual to Ising model) near its critical point. For large hexagon Wilson loops a perfect agreement is observed between the asymptotic EST expressions and the lattice MC results.

1 Introduction

1.1 Large Wilson loops and effective string theory

Historically, Wilson loops

$$W(C) = \left\langle \text{Tr} \exp \left[i \oint_C dx^\mu A_\mu(x) \right] \right\rangle \quad (1.1)$$

attracted attention in the context of the problem of the heavy-quark confinement although the full spectrum of problems where Wilson loops appear is much wider. Gauge theories whose Wilson loops (at least in some representations of the gauge group) obey area law [1]

$$\lim_{|C| \rightarrow \infty} \frac{1}{S(C)} \ln W(C) = -\sigma \neq 0 \quad (1.2)$$

(with $S(C)$ being the area of the surface spanned on contour C and with σ interpreted as the string tension) are often briefly called confining gauge theories.

However, the real problem of confinement is more general and can be reduced to area law (1.2) only under certain assumptions: heavy-quark limit, ignoring exceptional cases when the confining potential is not asymptotically linear and some other subtleties.

In eq. (1.2), the non-formal notation

$$|C| \rightarrow \infty \tag{1.3}$$

is used for the large-size limit of contour C , implying that the contour grows more or less uniformly in all directions. For brevity, we will often use expression *large Wilson loop*, keeping in mind the large-size limit $|C| \rightarrow \infty$ and not the value of the Wilson loop which is exponentially suppressed according to eq. (1.2). Typically, limit $|C| \rightarrow \infty$ assumes that area $S(C)$ and perimeter $L(C)$ of contour C scale as

$$S(C) \sim L^2(C) \rightarrow \infty. \tag{1.4}$$

In case of area law (1.2) condition (1.4) can be relaxed. On the other hand, the analysis of higher-order terms of the large-size expansion of $W(C)$ may require a more careful specification of details of the large-size limit (e.g. the uniform rescaling of contour C by a large factor).

The modern understanding of confining gauge theories is based on the idea that area law is a manifestation of a more fundamental phenomenon: effective-string formation (ESF) between static color charges separated by a large distance. The concept of ESF has a long history full of imprecise qualitative ideas, heuristic arguments and models without a solid theoretical basis. But finally it became clear that ESF is a phenomenon which allows for a systematic theoretical treatment. The phenomenon of ESF has many features similar to spontaneous breakdown of continuous symmetries. In particular, the large-distance (and low-energy) behavior of many quantities (including large Wilson loops) can be described by an effective string action that contains an infinite series of local terms ordered according to the counting of gradients similarly to the method of effective actions describing Goldstone modes in theories with a spontaneous breakdown of continuous symmetries. This approach to the description of ESF based on the effective action and on the large-size (or small-energy) expansion is usually called effective string theory (EST).

EST occupies a rather peculiar place in the large zoo of string-based theories:

- 1) EST is a systematic theory based on the expansion in a small parameter, inverse size of the string (or small energy of string excitations).
- 2) EST is not a fundamental string theory. It is an effective theory which can be applied only in the large-size limit.

The early time of EST was intertwined with the history of other stringy models and theories for hadrons. As for the problem of confinement, the string interpretation was emphasized by K. Wilson [1] combining intuitive arguments with the properties of the strong coupling expansion in lattice gauge theories. G. 't Hooft [2], [3] constructed a classification of states of non-abelian gauge theories in a finite periodic box. This classification combined with the limit of large volume puts the concept of *closed* periodic strings in confining gauge

theories on a solid theoretical ground. *Open* confining strings are associated with pairs of external static color charges and are described by Wilson loops. EST describes open and closed strings using the same effective action (up to extra boundary terms which are essential for higher-order corrections to Wilson loops and to the spectrum of open strings). M. Lüscher, G. Münster, K. Symanzik and P. Weisz [4]-[6] made several crucial steps on the way from naive string models towards EST as a systematic effective theory. The subsequent theoretical work in EST went in various directions including

- derivation of general constraints on terms appearing in the action of EST [7]-[15],
- computation of loop corrections in EST for rectangular Wilson loops [15], [17]-[20] and for other closely related quantities like correlation functions of Polyakov loops and spectra of closed and open strings [7], [9]-[14],
- analysis of string finite-width effects [6], [21], [22].

The predictions of EST have been successfully verified by many lattice MC tests (see review [23], recent publications [15], [24]-[28] and references therein).

One should keep in mind that the stringy interpretation for Wilson loops appears not only in the context of the large-size limit but also in other approaches: $1/N$ -expansion [29]-[32], large- D limit (D being the space-time dimension) [33]-[36], Regge limit [36]-[38]. Wilson loops attract much attention in superconformal theories (like 4D $\mathcal{N} = 4$ supersymmetric Yang-Mills theory), especially in the combination with the large- N limit and with the AdS/CFT correspondence [39]-[43], including the case of null polygonal Wilson loops [44]-[49] and tests of EST in holographic backgrounds [9], [10]. But these interesting fields of research are beyond the scope of this work where EST is understood as an effective theory relevant for the construction of the large-size expansion in confining gauge theories with area law (1.2) without assuming extra small parameters or extra symmetries.

1.2 Reduction of large Wilson loops to Laplace determinants in EST

EST is an effective theory. Its power is limited. For example, string tension σ appearing in area law (1.2) is determined by microscopic gauge theory (MGT) and cannot be computed in EST. Therefore EST provides incomplete information about large-size expansion of *single Wilson loops*. However, the large-size limit of certain *combinations of several Wilson loops* is completely computable in EST.

Let us take a set of *smooth* flat contours C_i ($1 \leq i \leq n$). Let us assign some number m_i to each contour C_i so that perimeters $L(C_i)$ and areas $S(C_i)$ of these contours obey constraints

$$\sum_{i=1}^n m_i = 0, \tag{1.5}$$

$$\sum_{i=1}^n m_i L(C_i) = 0, \quad (1.6)$$

$$\sum_{i=1}^n m_i S(C_i) = 0. \quad (1.7)$$

Now let us rescale each contour $C_i \rightarrow \lambda C_i$ by a large common factor λ . Then EST leads to the following expression for the large-size limit:

$$\lim_{\lambda \rightarrow \infty} \prod_{i=1}^n [W(\lambda C_i)]^{m_i} = \left\{ \prod_{i=1}^n \{\text{Det}_\zeta[-\Delta(C_i)]\}^{m_i} \right\}^{-(D-2)/2}. \quad (1.8)$$

Here $\Delta(C_i)$ is Laplace operator defined in the two-dimensional region bounded by contour C_i with Dirichlet boundary condition. D is the dimension of space-time. Notation $\text{Det}_\zeta[-\Delta(C_i)]$ stands for the determinant of operator $-\Delta(C_i)$ in ζ -regularization scheme (see sec. 4). In this paper we usually assume ζ -regularization for Laplace determinants although in many (but not in all) formulas one has a wider freedom of choice for the renormalization scheme.

Constraints (1.5) – (1.7) are imposed in order to cancel those contributions to the large-size expansion which are controlled by MGT but not by EST. For example, condition (1.7) cancels the σ dependence in the product on the LHS of (1.8).

Asymptotic formula (1.8) is a direct consequence of the results obtained in ref. [4]. The derivation of eq. (1.8) is briefly discussed in sec. 2. The basic idea is that in the limit of large size, Wilson loop $W(C)$ can be approximated by a functional integral over surfaces bounded by contour C . The large size of the contour justifies the steepest-descent expansion of this functional integral so that the problem reduces to finding the minimum of the action (minimal surface bounded by contour C) and to computing the determinant of the quadratic part of the action for fluctuations near this minimal surface. For flat contours C the contribution of fluctuations is described by the determinant of Laplace operator $\Delta(C)$ acting in the region bounded by C (with Dirichlet boundary condition). In D -dimensional space-time one has $D - 2$ transverse directions for the fluctuations of the string surface which explains power $-(D - 2)/2$ of Laplace determinant on the RHS of (1.8).

A remarkable feature of asymptotic formula (1.8) is that the RHS is independent of the gauge group (as long as we deal with a confining gauge theory and ESF stands behind the confinement) and the dependence on space-time dimension reduces to power $-(D - 2)/2$.

1.3 Case of polygonal Wilson loops

The above discussion of asymptotic formula (1.8) assumed that all contours C_i are smooth. But when it comes to lattice tests of EST, one has to deal with polygonal contours C_i . Eq. (1.8) still works for polygonal contours C_i if one

imposes an extra condition in addition to constraints (1.5) – (1.7). This extra constraint is needed because some properties of Wilson loops near the vertices of polygons are controlled by MGT and are not computable in EST: each vertex contributes an EST-non-controllable factor depending on the vertex angle. In order to cancel these factors on the LHS of (1.8) let us choose some set of angle values $\{\theta_a\}$ and let us distribute the angles from this common set $\{\theta_a\}$ between different polygons C_i in a “balanced way”. Let p_{ia} be the number of occurrences of angle value θ_a among vertices of polygon C_i (so that possible values are $p_{ia} = 0, 1, 2, \dots$). Then the vertex balance constraint reads

$$\sum_{i=1}^n m_i p_{ia} = 0. \quad (1.9)$$

If this condition is added to constraints (1.5) – (1.7) then one can use asymptotic formula (1.8) for polygonal contours. In case of flat polygonal contours condition (1.5) can be derived from condition (1.9) (see sec. 2.4). Therefore for the validity of asymptotic formula (1.8) it is sufficient to impose only constraints (1.6), (1.7) and (1.9).

If one omits area constraint (1.7) but still keeps constraints (1.6), (1.9) then eq. (1.8) can be generalized to the form (see sec. 2.3)

$$\left[\exp \left(\lambda^2 \sigma \sum_{i=1}^n m_i S(C_i) \right) \right] \prod_{i=1}^n [W(\lambda C_i)]^{m_i} \stackrel{\lambda \rightarrow \infty}{\equiv} \left\{ \prod_{i=1}^n \{ \text{Det}_\zeta [-\Delta(C_i)] \}^{m_i} \right\}^{-(D-2)/2} [1 + O(\lambda^{-2})]. \quad (1.10)$$

Our guiding principle for building the product of Wilson loops on the LHS of eq. (1.8) was to make such a combination of Wilson loops that its limit $\lambda \rightarrow \infty$ is completely determined by EST and is independent of the details of the MGT. Eq. (1.10) is written for a relaxed set of constraints: we have omitted condition (1.7). The price is that relation (1.10) contains string tension σ which cannot be computed in EST and is determined by MGT. Note that parameter σ appearing in (1.10) is the same as in area law (1.2). This statement is nontrivial because it assumes that Laplace determinants on the RHS of eq. (1.10) are taken in the ζ -regularization. In fact, what is important is not ζ -regularization itself but its property that power divergences vanish in ζ -regularization (similarly to the dimensional regularization).

1.4 Large-size expansion for single Wilson loops

The above presentation (1.8), (1.10) of EST results in terms of *products of Wilson loops*, whose large-size limit is either completely or almost completely under control of EST, is determined by our final aim: lattice MC tests of EST for polygonal Wilson loops. But for the derivation of asymptotic relations (1.8),

(1.10) one needs the large- λ expansion for a *single* Wilson loop:

$$\ln W(\lambda C) \stackrel{\lambda \rightarrow \infty}{\cong} f_{\ln}(C) \ln \lambda + \sum_{k \geq -2} \lambda^{-k} f_k(C) . \quad (1.11)$$

Here $f_{\ln}(C)$ and $f_k(C)$ are some functionals of contour C . These functionals are partly computable in EST but still are partly dependent on MGT. Large- λ expansion (1.11) is discussed in detail in sec. 2.2. At the moment it is important that the MGT sensitivity of expansion (1.11) cancels completely in eq. (1.8) and almost completely (up to the σ dependence) in eq. (1.10) if one imposes the corresponding set of constraints (1.5) – (1.7), (1.9).

The formal mathematical structure of large- λ expansion (1.11) is rather general. We have an asymptotic power series with an extra logarithmic term. Functionals $f_k(C)$ have obvious properties

$$f_k(\lambda C) = \lambda^{-k} f_k(C) \quad (k \neq 0) , \quad (1.12)$$

$$f_0(\lambda C) = f_0(C) + f_{\ln}(C) \ln \lambda , \quad (1.13)$$

$$f_{\ln}(\lambda C) = f_{\ln}(C) . \quad (1.14)$$

Expansion (1.11) represents the current understanding of EST and generalizes the results for loop corrections in EST which have been computed or at least studied. In principle, apart from the logarithmic term $f_{\ln}(C) \ln \lambda$, in higher orders of this expansion other “non-analytical” terms are not excluded.

The role of constraints (1.5) – (1.7), (1.9) assumed for the validity of eq. (1.8) is to cancel the contribution of λ -growing terms to eq. (1.8)

$$\sum_{i=1}^n m_i f_k(C_i) = 0 \quad (k = -1, -2, \ln) . \quad (1.15)$$

Then eq. (1.8) becomes equivalent to

$$\sum_{i=1}^n m_i f_0(C_i) = -\frac{D-2}{2} \sum_{i=1}^n m_i \ln \text{Det}_{\zeta} [-\Delta(C_i)] . \quad (1.16)$$

Explicit EST expressions for functionals $f_k(C_i)$ can be found in sec. 2.2. Note that

$$f_1(C) = 0 \quad (1.17)$$

(see sec. 2.5). This explains the $O(\lambda^{-2})$ correction on the RHS of eq. (1.10) coming from the term $\lambda^{-2} f_2(C)$ of expansion (1.11).

1.5 Lattice tests of effective string theory

Nowadays EST has the status of a mature theory. However, EST is an effective theory, EST can be used only in cases when the phenomenon of ESF occurs. But EST cannot tell us whether we really have ESF in a given microscopic gauge

theory or not. Also keep in mind that ESF is not the only possible mechanism of confinement. Therefore lattice MC tests of EST play an important role. Lattice MC simulations are also helpful for testing the internal kitchen of EST because some arguments used in EST (e.g. some constraints on higher-order terms of the effective action or the assumption that in the large-size limit we effectively deal with a pure bosonic string without extra fields living on the string world sheet) cannot be considered as rigorous theorems. Last but not least: inconsistencies observed in lattice MC simulations may trigger detecting errors in EST theoretical calculations as it happened with the two-loop EST correction $f_2(C)$ for rectangular Wilson loops (see sec. 2.5).

Anyway, EST has successfully passed through many lattice MC tests. These tests go far beyond Wilson loops and also include such quantities as correlation functions of Polyakov loops, the confining potential, the spectrum of closed and open strings, etc. The reader interested in general lattice tests of EST beyond the special case of Wilson loops (which make the subject of this paper) is referred to recent publications [23], [27], [28] and to references therein.

In case of Wilson loops, MC tests of EST asymptotic formulas (1.8), (1.10) have much freedom of choice:

- gauge group,
- space-time dimension,
- maximal order of EST corrections taken into account,
- shape of the Wilson contour.

For *rectangular* Wilson loops, EST has been successfully checked by lattice MC tests with high accuracy resolving higher-order corrections of the large- λ expansion. In particular, in case of 3D \mathbb{Z}_2 gauge theory high-precision MC results of ref. [15] confirmed EST correction $\lambda^{-3} f_3(C)$ coming from the boundary part of the effective action (see sec. 2.5).

The aim of this work is to test EST for Wilson loops with *non-rectangular polygonal* contours. In case of large non-rectangular contours, EST starts to work at rather large sizes of polygons, which imposes rather severe requirements on computer resources. Therefore concentrating on the problem of non-rectangular contours one has to sacrifice other degrees of freedom in lattice tests: the current work deals with

- the minimal non-trivial case of $D = 3$ space-time dimensions,
- the simplest gauge group \mathbb{Z}_2 (near its critical point where a full-fledged continuous quantum field theory is generated).

Another price that one has to pay for working with non-rectangular polygons is an insufficient accuracy of MC results, which makes difficult testing higher-order terms of the EST large-size expansion.

1.6 Structure of the paper

Sections 2 – 4 contain a review of well-known facts needed for understanding the main part of this work. In sec. 2 a brief derivation of asymptotic EST formulas (1.8), (1.10) is sketched. Sec. 3 describes basic properties of lattice 3D \mathbb{Z}_2 gauge theory and the duality of this theory to 3D Ising model. Sec. 4 is devoted

to determinants of two-dimensional Laplace operators. The computation of Laplace determinants needed for the comparison of MC results with EST is described in Appendix.

In sec. 5 we discuss the optimal choice of polygons for MC lattice tests of EST. In sec. 6 our lattice results are summarized and compared with EST.

Expert readers interested in the immediate comparison of lattice MC results with EST predictions may jump directly to Table 2 and to the content of sec. 6.3 which provides a simple but incomplete analysis of results. Sec. 6.4 contains a more thorough analysis of data by combining the results of this work with the high-precision value for the string tension σ of 3D \mathbb{Z}_2 gauge theory from ref. [15].

2 Wilson loops in EST

2.1 Basic ideas

As already mentioned above, the main idea of EST is that in systems where ESF occurs, low-energy and large-distance properties of the effective string can be described by an effective string action. The implementation of this idea is analogous to systems with a spontaneous breakdown of continuous symmetries:

- Identify low-energy degrees of freedom corresponding to the broken symmetry (partial breakdown Poincaré group in case of ESF).
- Write the most general action containing all terms compatible with the symmetries of the microscopic gauge theory.
- Effective Lagrangian is an infinite series of terms ordered according to the counting of gradients.
- All terms compatible with the symmetries of the microscopic gauge theory are allowed (but at a deeper level of the analysis certain constraints may be derived).
- This effective action allows to compute systematically low-energy and large-distance expansions for various quantities. In particular, large-size expansion (1.11) can be constructed for Wilson loops.
- Although the effective action contains an infinite amount of terms, for the computation of any given order of the large-size expansion only a finite amount of terms of the effective action is needed.
- Coefficients accompanying the terms of the effective action are typically determined by the microscopic theory and cannot be computed in EST. However, symmetries and general principles of quantum field theory may impose certain constraints on these coefficients.
- Loop diagrams of the effective theory may contain ultraviolet divergences.

From the physical point of view these divergences must be cut at the boundary of the applicability of the effective theory. However, technically in practical computations the formal treatment of these divergences has many common features with the usual renormalization.

2.2 One-loop expression for $W(C)$ in EST

The idea that in some limit Wilson loops $W(C)$ can be approximated by the functional integral over surfaces Σ whose boundary is fixed at Wilson contour C

$$W(C) \rightarrow \text{const} \int_{\partial\Sigma=C} D\Sigma \exp(-S_{\text{EST}}[\Sigma]) . \quad (2.1)$$

has a long history [50]. The detailed implementation of this idea depends on which asymptotic limit is assumed: large-size [4] or large- N [31], [32]. As was already mentioned, the large- N case is not related to the content of this work but it is an interesting case, especially when the large- N limit is combined with supersymmetry and with AdS/CFT correspondence.

The large-size limit allows to arrange the effective string action $S_{\text{EST}}[\Sigma]$ as an infinite series of terms according to the counting of gradients. The leading-order part of EST action is Nambu action

$$S_{\text{EST}}(\Sigma) = \sigma_0 A(\Sigma) + \dots \quad (2.2)$$

Here $A(\Sigma)$ is the area of Σ , σ_0 is the bare string tension. Generally one should distinguish between bare string action σ_0 appearing in (2.2) and the physical string tension σ appearing in area law (1.2). But in some regularizations automatically removing power divergences (e.g. dimensional and ζ regularizations) the difference between σ_0 and σ is not visible in the computation of the first orders of the large-size expansion.

The case when one approximates $S_{\text{EST}}(\Sigma)$ by Nambu action $\sigma_0 A(\Sigma)$ and computes (2.1) in one-loop approximation using the steepest-decent method was studied in ref. [4] for smooth contours C . Below we briefly sketch the generalization of results of ref. [4] to the case of flat *polygonal* contours.

For the computation of the first orders of the large-size expansion of Wilson loops, the next-to-Nambu corrections in eq. (2.2) are irrelevant so that one has to compute

$$\int_{\partial\Sigma=C} D\Sigma \exp[-\sigma_0 A(\Sigma)] . \quad (2.3)$$

Surface area defining Nambu action can be represented in the form

$$A(\Sigma) = \int_U du^1 du^2 \sqrt{\det_{a,b}(Q_{ab})} , \quad (2.4)$$

$$Q_{ab} = \sum_{\mu,\nu=1}^D \frac{\partial X^\mu}{\partial u^a} \frac{\partial X^\mu}{\partial u^b} . \quad (2.5)$$

Nambu action is reparametrization invariant. Therefore in EST (like in the theory of fundamental boson strings) reparametrization invariance must be treated as a gauge symmetry. In case of flat Wilson contours C , it is convenient to use the planar gauge (sometimes called static gauge):

$$u^a = X^a \quad (a = 1, 2) , \quad (2.6)$$

$$X^\perp = X^\perp (X^1, X^2) \quad (\perp = 3, 4, \dots, D). \quad (2.7)$$

In this gauge

$$Q_{ab} = \delta_{ab} + \sum_{k=3}^D \frac{\partial X^k}{\partial X^a} \frac{\partial X^k}{\partial X^b}, \quad (2.8)$$

In quadratic approximation

$$\sqrt{\det_{a,b}(Q_{ab})} = 1 + \frac{1}{2} \sum_{a=1}^2 \sum_{k=3}^D \frac{\partial X^k}{\partial X^a} \frac{\partial X^k}{\partial X^a} + \dots \quad (2.9)$$

$$\iint_U dX^1 dX^2 \sqrt{\det_{a,b}(Q_{ab})} = S(C) + \frac{1}{2} \iint_U dX^1 dX^2 \sum_{a=1}^2 \sum_{k=3}^{D-2} \frac{\partial X^k}{\partial X^a} \frac{\partial X^k}{\partial X^a}, \quad (2.10)$$

$$\partial U = C. \quad (2.11)$$

The steepest-descent integration yields

$$\int_{\partial\Sigma=C} D\Sigma \exp[-\sigma_0 A(\Sigma)] = \text{const} [\text{Det}_{\text{reg}}[-\Delta(C)]]^{-(D-2)/2} \exp[-\sigma_0 S(C)]. \quad (2.12)$$

For polygonal contours Laplace determinant has area, perimeter and cusp divergences so that the regularized and renormalized Laplace determinants are connected by the relation

$$\text{Det}_{\text{reg}}[-\Delta(C)] = \exp[a_2 S(C) + a_1 L(C) + a_0(C)] \text{Det}_{\text{ren}}[-\Delta(C)]. \quad (2.13)$$

Explicit expressions for these divergences in proper-time regularization are given by eq. (4.6). In ζ -regularization, power divergences a_1, a_2 vanish and one is left only with the cusp divergence $a_0(C)$

$$\zeta\text{-regularization: } a_1 = 0, \quad a_2 = 0. \quad (2.14)$$

After the renormalization one arrives at the asymptotic expansion

$$W(C) \stackrel{|C| \rightarrow \infty}{\equiv} K \left[\prod_{\gamma=1}^{M(C)} B(\theta_\gamma) \right] \exp[-\sigma S(C) + \rho L(C)] \\ \times [\text{Det}_\zeta(-\Delta(C))]^{-(D-2)/2} (1 + \dots). \quad (2.15)$$

We use ζ -renormalization scheme for the renormalized Laplace determinant. In principle, other renormalization schemes could be also used up to some subtleties:

1) In the final part of our work we will need explicit expressions for Laplace determinants on hexagons which will be computed using general expressions of ref. [51] where Laplace determinants were computed in the ζ -regularization scheme.

2) ζ -regularization has important properties (2.14), (4.11). They allow to identify parameter σ appearing in eq. (2.15) with the physical string tension.

In eq. (2.15), θ_γ are interior vertex angles of the polygon. $M(C)$ is the number of vertices of the polygon.

Parameters K, ρ, σ and function $B(\theta_\gamma)$ appearing on the RHS of eq. (2.15) are determined by the dynamics of the microscopic gauge theory and cannot be computed in EST. For flat polygons C , sum rule

$$\sum_{\gamma} \frac{\pi - \theta_{\gamma}}{2\pi} = 1 \quad (2.16)$$

allows to minimize the amount of unknown factors (not controlled by EST) by redefining

$$\tilde{B}(\theta_{\gamma}) = \left[B(\theta_{\gamma}) K^{(\pi - \theta_{\gamma})/(2\pi)} \right]$$

so that

$$K \left[\prod_{i=1}^{M(C)} B(\theta_{\gamma}) \right] = \prod_{i=1}^{M(C)} \tilde{B}(\theta_{\gamma}) . \quad (2.17)$$

On the other hand, coefficient K provides a natural way to represent the freedom of normalization of Wilson loops in the microscopic gauge theory.

Combining eq. (2.15) with scaling property (4.11) of $\text{Det}_{\zeta}[-\Delta(\lambda C)]$ we arrive at area law (1.2). This means that parameter σ appearing in eq. (2.15) has the meaning of the ‘‘observable’’ physical string tension.

Using property (4.10) of Laplace determinant in ζ -regularization and eq. (4.3), we can rewrite (2.15) in the form

$$\begin{aligned} \ln W(\lambda C) \stackrel{\lambda \rightarrow \infty}{\cong} & \ln \left(\prod_{i=1}^{M(C)} \tilde{B}(\theta_{\gamma}) \right) - \sigma \lambda^2 S(C) + \rho \lambda L(C) \\ & + \frac{D-2}{2} \left\{ \sum_{\gamma=1}^{M(C)} \xi(\theta_{\gamma}) \ln \lambda - \ln [\text{Det}_{\zeta}(-\Delta(C))] \right\} + O(\lambda^{-2}) \end{aligned} \quad (2.18)$$

where function $\xi(\theta)$ is given by eq. (4.3). The status of the higher-order corrections starting from $O(\lambda^{-2})$ will be discussed in sec. 2.5.

Thus we have the following structure of the large- λ expansion corresponding to the first terms of the general expansion (1.11):

$$\ln W(\lambda C) \stackrel{\lambda \rightarrow \infty}{\cong} f_{\text{ln}}(C) \ln \lambda + \lambda^2 f_{-2}(C) + \lambda f_{-1}(C) + f_0(C) + O(\lambda^{-2}) \quad (2.19)$$

where

$$f_{\text{ln}}(C) = \frac{D-2}{2} \sum_{\gamma=1}^{M(C)} \xi(\theta_{\gamma}), \quad (2.20)$$

$$f_{-2}(C) = -\sigma S(C), \quad (2.21)$$

$$f_{-1}(C) = \rho L(C) , \quad (2.22)$$

$$f_0(C) = \ln \left(\prod_{i=1}^{M(C)} \tilde{B}(\theta_{\gamma_i}) \right) - \frac{D-2}{2} \ln [\text{Det}_{\zeta}(-\Delta(C))] . \quad (2.23)$$

2.3 Derivation of the asymptotic formula for a “balanced” product of Wilson loops

Now we turn to the derivation of eq. (1.10). As mentioned in the comments to eq. (1.10), we assume that we have several polygonal contours C_i and a set of numbers m_i obeying conditions (1.6). We also assume that vertex angles θ_{γ_i} of polygons C_i belong to a common set of angles $\{\theta_a\}$, angle θ_a appearing p_{ia} times in C_i with constraint (1.9). Then according to eq. (2.20)

$$\sum_i m_i f_{\ln}(C_i) = \frac{D-2}{2} \sum_i m_i \sum_{\gamma=1}^{M(C)} \xi(\theta_{\gamma_i}) . \quad (2.24)$$

Obviously

$$\sum_{\gamma=1}^{M(C)} \xi(\theta_{\gamma_i}) = \sum_a p_{ia} \xi(\theta_a) \quad (2.25)$$

so that

$$\sum_i m_i f_{\ln}(C_i) = \frac{D-2}{2} \sum_{a=1}^M \xi(\theta_a) \left(\sum_i m_i p_{ia} \right) . \quad (2.26)$$

Then constraint (1.9) leads to

$$\sum_i m_i f_{\ln}(C_i) = 0 . \quad (2.27)$$

Similarly we have

$$\sum_i m_i \ln \left(\prod_{\gamma=1}^{M(C_i)} \tilde{B}(\theta_{\gamma_i}) \right) = \sum_{a=1}^M (\ln \tilde{B}(\theta_a)) \left(\sum_i m_i p_{ia} \right) = 0 . \quad (2.28)$$

Now we find from eqs. (2.18), (2.27), (2.28)

$$\begin{aligned} & \sum_i m_i \ln W(\lambda C_i) \stackrel{\lambda \rightarrow \infty}{\cong} -\sigma \lambda^2 \sum_i m_i S(C_i) \\ & - \frac{D-2}{2} \sum_i m_i \ln [\text{Det}_{\zeta}(-\Delta(C_i))] + O(\lambda^{-2}) . \end{aligned} \quad (2.29)$$

This proves asymptotic formula (1.10) under assumptions (1.6), (1.9). If one adds area constraint (1.7) then eq. (1.10) simplifies to eq. (1.8).

2.4 Dependent constraint

Note that our derivation of eq. (2.29) for polygonal contours C_i did not use constraint (1.5). Technically we could avoid the involvement of eq. (1.5) by using reduction (2.17) but the real reason is that eq. (1.5) is a trivial consequence of constraint (1.9) and sum rule (2.16). Indeed, eq. (2.16) can be rewritten in the form

$$1 = \sum_a p_{ia} \frac{\pi - \theta_a}{2\pi} \quad (2.30)$$

which leads to

$$\sum_{i=1}^n m_i = \sum_{i=1}^n m_i \sum_a p_{ia} \frac{\pi - \theta_a}{2\pi} = \sum_a \frac{\pi - \theta_a}{2\pi} \sum_{i=1}^n m_i p_{ia}. \quad (2.31)$$

2.5 Higher orders of the large-size expansion

One-loop result (2.19) can be generalized to higher orders of the large- λ expansion according to eq. (1.11). A careful derivation of expansion (1.11) requires much work:

- 1) analysis of constraints on terms of the full EST action [7]-[15],
- 2) computation of diagrams generated by this effective action [15], [17]-[20].

As was already mentioned in eq. (1.17), $f_1(C) = 0$. The reason is that EST action contains two parts:

- surface action represented by a two-dimensional integral over the region bounded contour C (including Nambu action),
- boundary action represented by a one-dimensional integral over contour C [7], [10], [15]

The surface action generates terms $f_n(C)$ with even n . The boundary action also generates terms with odd n but only starting from $f_3(C)$. Hence neither surface nor boundary actions can generate $f_1(C)$.

One should be alerted about the traditional but somewhat confusing naming scheme for terms $f_n(C)$ of expansion (1.11). Terms $f_{2n}(C)$ are often called $(n+1)$ -loop corrections implying that these terms come from $(n+1)$ -loop diagrams with vertices generated by the surface terms of the effective action. This nomenclature ignores contributions from the boundary action, in particular terms $f_n(C)$ with odd n .

Correction $f_2(C)$ is in principle computable in EST but currently it is known only for rectangular Wilson contours C . This correction was computed for rectangular Wilson loops and for the correlation function of two Polyakov loops in refs. [17], [18]. The result of refs. [17], [18] for Polyakov loops was confirmed by a computation in another regularization [7]. However, the result of refs. [17], [18] for Wilson loops has an arithmetic error which was corrected in refs. [19], [20].

Correction $f_3(C)$ comes from the boundary part of the effective action. In case of the correlation function of two Polyakov lines this correction was com-

puted in ref. [10]. In case of rectangular Wilson loops the $f_3(C)$ term for was computed in EST and tested by lattice MC (in 3D \mathbb{Z}_2 gauge theory) in ref. [15].

3 Lattice \mathbb{Z}_2 gauge theory

3.1 \mathbb{Z}_2 gauge theory

High-precision tests of EST are often performed using \mathbb{Z}_2 gauge theory (sometimes called gauge Ising model) in $D = 3$ Euclidean space-time dimensions [15], [52], [53]. Discrete group \mathbb{Z}_2 contains two elements ± 1 . \mathbb{Z}_2 gauge theory is defined by the standard Wilson lattice action with link variables $U_l = \pm 1$. In particular, the partition function $Z_{\mathbb{Z}_2}$ of \mathbb{Z}_2 gauge theory is

$$Z_{\mathbb{Z}_2}(\beta_{\mathbb{Z}_2}) = \sum_{\{U_l\}} \exp \left[\sum_P \beta_{\mathbb{Z}_2} \Pi(P) \right]. \quad (3.1)$$

On the RHS, the external sum runs over all lattice link configurations $\{U_l\}$ with $U_l = \pm 1$. $\beta_{\mathbb{Z}_2}$ is lattice coupling constant, the sum in the exponent runs over all non-oriented plaquettes P , and $\Pi(P) = \pm 1$ is the product of link variables $U_l = \pm 1$ associated with four links P_i of plaquette P

$$\Pi(P) = \prod_{l \in P} U_l. \quad (3.2)$$

There are several reasons why 3D \mathbb{Z}_2 gauge theory is frequently used in lattice MC simulations:

1) Many predictions of EST are universal, i.e. independent of the gauge group [see e.g. eq. (1.8)]. Therefore in high-precision MC lattice tests of EST it is natural to choose the simplest but still nontrivial confining gauge theory. 3D \mathbb{Z}_2 gauge theory is the best candidate for this role.

2) $D = 3$ is the minimal space-time dimension where area law and EST are implemented nontrivially. At $D = 2$, non-Abelian gauge theories are exactly solvable, EST corrections to the area law are proportional to $D - 2$ (number of the transverse degrees of freedom) and vanish at $D = 2$.

3) Although \mathbb{Z}_2 group is Abelian, the \mathbb{Z}_2 lattice gauge theory has a confining phase.

4) 3D \mathbb{Z}_2 gauge theory is dual to 3D Ising model. This duality is crucial for understanding the confining properties and the continuous limit of 3D \mathbb{Z}_2 gauge theory. \mathbb{Z}_2 -Ising duality also plays an important role in high-efficiency algorithms of lattice MC simulations.

3.2 Duality of 3D Ising model and lattice \mathbb{Z}_2 gauge theory

3.2.1 Preliminary comments

This section contains a brief review of 3D \mathbb{Z}_2 -Ising duality. Before turning to technical details it makes sense to describe the main consequences of this duality.

1) 3D lattice \mathbb{Z}_2 gauge theory has confinement and deconfinement phases separated by a critical point. \mathbb{Z}_2 -Ising duality maps the confinement phase of \mathbb{Z}_2 theory to the spontaneously broken phase of Ising model whereas the \mathbb{Z}_2 deconfinement phase is mapped to the Ising non-broken phase.

2) Due to \mathbb{Z}_2 -Ising duality the critical point of \mathbb{Z}_2 theory belongs to the same universality class as the critical point of 3D Ising model. This critical point can be used for the construction of various continuous field theories. If the lattice theory is taken exactly at the critical point then its correlation functions have a power asymptotic behavior at large distances, which is controlled by the conformal field theory corresponding to this universality class.

However, if one slightly deviates from the critical point towards the confinement phase of \mathbb{Z}_2 theory (or towards the broken phase of Ising model) and combines the approach to the critical point with an appropriate rescaling of distances and momenta then one arrives at a quite physical full-fledged continuous quantum field theory with *massive* particles. This massive continuous quantum field theory exists in two essentially equivalent \mathbb{Z}_2 -based and Ising-based versions. In \mathbb{Z}_2 -representation, massive particles can be interpreted as “glueballs” whose spectrum can be measured by lattice MC [54]. Wilson loops of \mathbb{Z}_2 -based theory obey area law (1.2).

3) \mathbb{Z}_2 -Ising duality allows to interpret the confinement of \mathbb{Z}_2 gauge theory in terms of Ising model. In particular, the string tension of confining strings in \mathbb{Z}_2 theory is equal to the surface tension between two different spontaneously broken phases of Ising model. The \mathbb{Z}_2 -Ising duality provides a correspondence between correlation functions of the two dual theories. \mathbb{Z}_2 Wilson loops can be expressed via multi-spin correlation functions of Ising model.

4) One can also profit from the \mathbb{Z}_2 -Ising duality in lattice MC simulations. The computation of \mathbb{Z}_2 Wilson loops can be performed directly in Ising model. Numerical simulations in 3D Ising model have a long history. Powerful algorithms have been developed. In particular, for the computation of \mathbb{Z}_2 Wilson loops directly in the dual Ising model an extremely efficient hierarchical MC (HMC) algorithm was suggested and successfully applied (see sec. 3.2.5). One of the features of this method is that it allows to compute a ratio of two Wilson loops directly, without computing the two Wilson loops separately. Large Wilson loops make many problems in lattice MC computations. The possibility to avoid their separate computation and to work directly with ratios of Wilson loops allows to compute ratios of large Wilson loops in 3D \mathbb{Z}_2 gauge theory with an unprecedented accuracy.

3.2.2 Ising model

The partition function of Ising model is

$$Z_I(\beta_I) = \sum_{\{s_k\}} \exp \left[\beta_I \sum_{\{i,j\}: \text{next neighbors}} s_i s_j \right]. \quad (3.3)$$

The external sum on the RHS runs over all lattice site configurations $\{s_k\}$ with $s_k = \pm 1$. The sum in the exponent runs over links represented by non-ordered pairs $\{i, j\}$ of next-neighbor sites i, j . β_I is lattice coupling constant (inverse temperature in the classical interpretation of Ising model).

Ising model can be considered for arbitrary dimension D . As is well known, the 2D Ising model is exactly solvable. It is remarkable that the critical point of 2D Ising model was first computed using the duality by Kramers and Wannier [55] before Onsager [56] found the exact solution of the model (computing the free energy at arbitrary temperatures). The duality transformation maps high temperatures to low temperatures. In terms of inverse temperature β duality transformation $\beta_{I,2D} \rightarrow \beta'_{I,2D}$ is described by the relation

$$\sinh(2\beta'_{I,2D}) \sinh(2\beta_{I,2D}) = 1. \quad (3.4)$$

This transformation leaves the critical point of 2D Ising model intact:

$$\beta'_{I,2D} = \beta_{I,2D} = \beta_{I,2D}^{\text{crit}} \quad (3.5)$$

so that eq. (3.4) leads to the following value for the critical point:

$$\beta_{I,2D}^{\text{crit}} = \frac{1}{2} \ln(1 + \sqrt{2}). \quad (3.6)$$

The case of 3D Ising model is different: in spite of much invested effort no exact solution was found. But it is possible to extend the concept of duality to $D > 2$ [57] and to show that 3D Ising model is dual to lattice \mathbb{Z}_2 gauge theory [58] (see also review [59] and references therein).

3.2.3 Duality of 3D Ising model and \mathbb{Z}_2 gauge theory

3D \mathbb{Z}_2 lattice gauge theory with coupling constant $\beta_{\mathbb{Z}_2}$ (3.1) is dual to Ising model with coupling β_I if constants $\beta_{\mathbb{Z}_2}$ and β_I are connected by relation [58]

$$\sinh(2\beta_I) \sinh(2\beta_{\mathbb{Z}_2}) = 1, \quad (3.7)$$

which formally coincides with duality relation (3.4) for the self-dual 2D Ising model. But now we deal with a duality connecting two different models.

\mathbb{Z}_2 -Ising duality relations can be derived for many quantities (free energy, correlation functions), see refs. [58], [59]. For our work we need only the expression for Wilson loops of \mathbb{Z}_2 gauge theory via multi-spin correlation functions of Ising model [58], [59], [63], [64]. The Ising-model representation for the \mathbb{Z}_2 Wilson loop $W(C)$ can be constructed in several steps:

- 1) Choose some lattice surface S bounded by contour C of the Wilson loop (the choice of S is not important but for flat contours C it is natural to take the flat region bounded by C).
- 2) Select all next-neighbor Ising spin links crossing surface S (\mathbb{Z}_2 and Ising models live on dual lattices, i.e. links of the Ising model are in one-to-one correspondence to plaquettes of \mathbb{Z}_2 theory crossed by Ising links).

3) Change the sign of Ising coupling β_I for the selected links in the Gibbs distribution of Ising model.

4) Compute partition function Z_S corresponding to the Ising model with the above change of the spin couplings.

5) Normalize Z_S with respect to the usual Ising partition function Z . The result Z_S/Z is the Ising dual representation for Wilson loop $W(C)$ of \mathbb{Z}_2 theory:

$$W(C) = \frac{Z_S}{Z}. \quad (3.8)$$

In case of two Wilson loops eq. (3.8) leads to

$$\frac{W(C_1)}{W(C_2)} = \frac{Z_{S_1}}{Z_{S_2}}. \quad (3.9)$$

If $S_2 \subset S_1$ (i.e. contour C_1 encloses contour C_2) then eq. (3.9) can be rewritten as

$$\frac{W(C_1)}{W(C_2)} = \left\langle \exp \left[-2\beta_I \sum_{(i,j) \in D(S_1 \setminus S_2)} s_i s_j \right] \right\rangle_{S_2}. \quad (3.10)$$

Here $S_1 \setminus S_2$ is the complement of S_2 in S_1 . $D(S_1 \setminus S_2)$ is the set of Ising links dual to \mathbb{Z}_2 -lattice surface $S_1 \setminus S_2$. The sum in the exponent runs over pairs (i, j) of Ising neighbor sites which are dual to surface $S_1 \setminus S_2$. Notation $\langle \dots \rangle_{S_2}$ stands for averaging with the statistical weight corresponding to partition function Z_{S_2} .

3.2.4 Critical point

The critical point of 3D Ising model is known with a high precision [65]:

$$\beta_I^{\text{crit}} = 0.22165455(3). \quad (3.11)$$

Using duality relation (3.7), one finds the critical point of 3D \mathbb{Z}_2 gauge theory:

$$\beta_{\mathbb{Z}_2}^{\text{crit}} = 0.76141346(7). \quad (3.12)$$

3.2.5 Hierarchical MC algorithm for ratios of large Wilson loops

Lattice tests of EST must deal with Wilson loops of large size. A straightforward MC computation of large Wilson loops requires computer time increasing exponentially with growth of the area of the Wilson loop. The problem of this exponential growth is partly solved by Lüscher-Weisz algorithm [66], [67] which can be used for any gauge group. In case of lattice \mathbb{Z}_2 gauge theory another high-efficiency algorithm was suggested in ref. [68]. In applications to Wilson loops this algorithm is well described in ref. [20].

This algorithm is based on several ideas.

1) If one is interested in a MC computation of a ratio of two large Wilson loops $W(C)/W(C')$ then one should compute this ratio directly without splitting the problem in separate MC computations of $W(C)$ and $W(C')$.

2) One should profit from \mathbb{Z}_2 -Ising duality relation (3.10) and perform the MC simulation in the dual Ising model.

3) Instead of the direct computation of $W(C)/W(C')$ in Ising model using eq. (3.10), first rearrange this ratio

$$\frac{W(C)}{W(C')} = \frac{W(C_0)W(C_1)}{W(C_1)W(C_2)} \cdots \frac{W(C_{n-1})W(C_n)}{W(C_n)W(C_{n+1})}, \quad (3.13)$$

$$C_0 = C, \quad C_{n+1} = C'. \quad (3.14)$$

Auxiliary contours C_1, \dots, C_n must be chosen so that for all i contours C_i and C_{i+1} are rather close and ratios $W(C_i)/W(C_{i+1})$ do not deviate too much from 1 (i.e. one should avoid exponentially large or exponentially small ratios $W(C_i)/W(C_{i+1})$). In this case each auxiliary ratio $W(C_i)/W(C_{i+1})$ can be computed without problems by MC simulations in Ising model using eq. (3.10). In short, hierarchical MC (HMC) algorithm may be written in the form (in case $S_{m+1} \subset S_m$)

$$\left[\frac{W(C)}{W(C')} \right]^{\text{HMC}} = \prod_{m=0}^n \left\langle \exp \left[-2\beta_I \sum_{(i,j) \in D(S_m \setminus S_{m+1})} s_i s_j \right] \right\rangle_{S_{m+1}}^{\text{MC}}. \quad (3.15)$$

4 2D Laplace determinants

4.1 Ultraviolet divergences and renormalization

In order to use EST asymptotic formulas (1.8), (1.10) for large Wilson loops, we need Laplace determinants. We use notation $\Delta(C)$ for Laplace operator defined in a flat region bounded by contour C with Dirichlet boundary condition.

Ultraviolet divergences of 2D Laplace determinants are controlled by the heat-kernel expansion [4], [69]-[73]:

$$\text{Tr} e^{t\Delta(C)} = \frac{1}{4\pi t} S(C) - \frac{1}{8\sqrt{\pi t}} L(C) - \frac{1}{2} \delta(C) + O(t^{1/2}). \quad (4.1)$$

For smooth contours C the t^0 term of this expansion is given by

$$\delta(C) = -\frac{1}{3}. \quad (4.2)$$

For polygonal contours C

$$\delta(C) = - \sum_{\gamma=1}^{M(C)} \xi(\theta_\gamma), \quad (4.3)$$

Here θ_γ are interior polygon angles and

$$\xi(\theta) = \frac{\pi^2 - \theta^2}{12\pi\theta}. \quad (4.4)$$

For cusp function $\xi(\theta)$, an integral representation was found by M. Kac in ref. [70]. Simplified expression (4.4) for $\xi(\theta)$ was obtained by D. B. Ray (the derivation is described in ref. [74]).

In the proper-time regularization

$$\ln \text{Det}_\tau [-\Delta (\lambda C)] = - \int_\tau^\infty \frac{dt}{t} \text{Tr} e^{t\Delta(C)} \quad (4.5)$$

at $\tau \rightarrow 0$ one has divergences

$$\ln \text{Det}_\tau [-\Delta (\lambda C)] \stackrel{\tau \rightarrow 0}{\equiv} -\frac{1}{4\pi\tau} S(C) + \frac{1}{4\sqrt{\pi\tau}} L(C) - \frac{1}{2} \delta(C) \ln \tau + O(\tau^0) . \quad (4.6)$$

In ζ -regularization method, one first defines the regularizing ζ -function at $\text{Re } s > 2$

$$Z_C(s) = \text{Sp} [(-\Delta(C))^{-s}] = \frac{1}{\Gamma(s)} \int_0^\infty dt t^{s-1} \text{Tr} e^{t\Delta(C)} . \quad (4.7)$$

Then one performs the analytical continuation to $s = 0$ ($Z_C(s)$ is regular at $s = 0$) and computes the derivative

$$Z'_C(s) \equiv \frac{d}{ds} Z_C(s) . \quad (4.8)$$

The determinant in the ζ -regularization is

$$\text{Det}_\zeta [-\Delta(C)] = \exp [-Z'_C(0)] . \quad (4.9)$$

Laplace determinant in ζ -regularization has properties

$$\ln \text{Det}_\zeta [-\Delta(\lambda C)] = \delta(C) \ln \lambda + \ln \text{Det}_\zeta [-\Delta(C)] , \quad (4.10)$$

$$\text{Det}_\zeta [-\Delta(\lambda C)] = \lambda^{\delta(C)} \text{Det}_\zeta [-\Delta(C)] . \quad (4.11)$$

Using eqs. (2.15), (4.3), (4.4), (4.11), we obtain coefficient $f_{\text{ln}}(C)$ appearing in large-size expansion (2.19)

$$f_{\text{ln}}(C) = -\frac{D-2}{2} \delta(C) = (D-2) \sum_{\gamma=1}^{M(C)} \frac{\pi^2 - \theta_\gamma^2}{24\pi\theta_\gamma} . \quad (4.12)$$

4.2 Computation of 2D Laplace determinants

As is well known, Laplace determinants in 2D regions can be computed using the conformal anomaly [75]-[78]. In order to compute Laplace determinant $\text{Det}(-\Delta(C))$ for the region bounded by contour C , one has to construct a conformal mapping of this region to some standard region (semiplane or circle). In case of polygons this conformal mapping is given by Schwarz-Christoffel (SC)

transformation. Thus combining the conformal anomaly and SC transformation, one can compute Laplace determinants for arbitrary polygons. However, on this way one must solve two problems:

- the anomaly-based representation for Laplace determinants has an integral form and this integral must be computed,
- this integral representation has cusp divergences which must be renormalized.

These problems were successfully solved by E. Aurell and P. Salomonson in ref. [51] where 2D Laplace determinant with Dirichlet boundary condition for an arbitrary polygon was expressed via parameters of SC mapping. In Appendix we apply the general results of ref. [51] to the computation of Laplace determinants $\text{Det}_\zeta [-\Delta (H_{n,m})]$ for hexagon contours $H_{n,m}$ (5.2) which are needed for the EST analysis of our MC results for Wilson loops. The final numerical results for $\text{Det}_\zeta [-\Delta (H_{n,m})]$ are listed in Table 4 of Appendix.

5 Choice of polygons for lattice tests EST

5.1 Hexagons $H_{n,m}$

Using EST, one can construct the large-size expansion for Wilson loops with any polygonal contours. But when it comes to lattice tests of EST, the choice of polygons is constrained by several factors. The cubic lattice allows for polygons with angles $\pi/2$ and $3\pi/2$ only. EST has been well tested for rectangular Wilson loops. If one goes beyond rectangles then the simplest polygon with all vertex angles being $\pi/2$ or $3\pi/2$ is a non-convex hexagon containing one vertex with angle $3\pi/2$ and five vertices with angles $\pi/2$.

Any polygon can be described by the cyclic sequence of side its lengths l_i and interior vertex angles $\alpha_{i,i+1}$ between sides with lengths l_i and l_{i+1}

$$P(l_1, \alpha_{1,2}, l_2, \alpha_{2,3}, \dots, l_n, \alpha_{n,1}) . \quad (5.1)$$

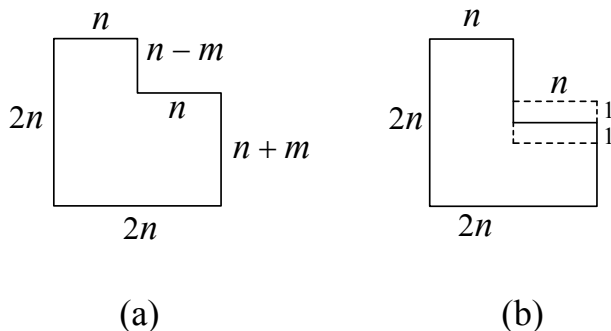


Figure 1: (a) Hexagon $H_{n,m}$. (b) Hexagon $H_{n,0}$ (solid) and its deformations (dashed) to $H_{n,1}$ and $H_{n,-1}$

In this paper we work with hexagons (Fig. 1a)

$$H_{n,m} = P \left(2n, \frac{\pi}{2}, 2n, \frac{\pi}{2}, n, \frac{\pi}{2}, n-m, \frac{3\pi}{2}, n, \frac{\pi}{2}, n+m, \frac{\pi}{2} \right). \quad (5.2)$$

These polygons have perimeter

$$L(H_{n,m}) = 8n \quad (5.3)$$

and area

$$S(H_{n,m}) = (3n+m)n. \quad (5.4)$$

For these hexagons one can define ratios of Wilson loops

$$q_{n,m}^{\pm} = \left[\frac{W(H_{n,0})}{W(H_{n,\pm m})} \right]^{\pm 1}, \quad (5.5)$$

$$r_{n,m} = \frac{W(H_{n,-m})W(H_{n,m})}{[W(H_{n,0})]^2} = \frac{q_{n,m}^-}{q_{n,m}^+}. \quad (5.6)$$

Ratios $q_{n,m}^{\pm}$, $r_{n,m}$ are special cases of the general product

$$\prod_{i=1}^n [W(C_i)]^{m_i} \quad (5.7)$$

obeying conditions of perimeter and angle balance conditions (1.6), (1.9). In addition, ratios $r_{n,m}$ obey area balance condition (1.7).

In the large-size uniform rescaling limit according to (1.10)

$$q_{jn,jm}^{\pm} \stackrel{j \rightarrow \infty}{\cong} e^{\sigma j^2 mn} \left[\frac{\text{Det}_{\zeta}[-\Delta(H_{n,\pm m})]}{\text{Det}_{\zeta}[-\Delta(H_{n,0})]} \right]^{\pm(D-2)/2} [1 + O(j^{-2})], \quad (5.8)$$

$$r_{jn,jm} \stackrel{j \rightarrow \infty}{\cong} \left\{ \frac{\text{Det}_{\zeta}[-\Delta(H_{n,0})]}{\sqrt{\text{Det}_{\zeta}[-\Delta(H_{n,m})] \text{Det}_{\zeta}[-\Delta(H_{n,-m})]}} \right\}^{D-2} [1 + O(j^{-2})]. \quad (5.9)$$

In case of \mathbb{Z}_2 gauge theory, the lattice computation based on HMC algorithm (see sec. 3.2.5) assumes an independent computation of $q_{n,m}^-$ and $q_{n,m}^+$. Finally $r_{n,m}$ can be expressed via $q_{n,m}^{\pm}$ using eq. (5.6).

In the case of hexagons $H_{n,m}$ (5.2) we find from eqs. (4.3), (4.4)

$$\delta(H_{n,m}) = -\frac{5}{9}. \quad (5.10)$$

Combining this with (4.10), we obtain

$$\ln \text{Det}_{\zeta}[-\Delta(H_{jn,jm})] = -\frac{5}{9} \ln j + \ln \text{Det}_{\zeta}[-\Delta(H_{n,m})]. \quad (5.11)$$

Setting $m = 0$, we find

$$\ln \text{Det}_{\zeta}[-\Delta(H_{n,0})] = \ln \text{Det}_{\zeta}[-\Delta(H_{1,0})] - \frac{5}{9} \ln n. \quad (5.12)$$

5.2 Modified large-size limit

From the theoretical point of view, the uniform rescaling limit

$$m, n \rightarrow \infty, \quad m/n = \text{const} \quad (\text{uniform limit}) \quad (5.13)$$

for ratios $q_{n,m}^\pm$, $r_{n,m}$ is the simplest version of the large-size limit for EST [see eqs. (5.8), (5.9)]. However, when it comes to lattice tests of EST in 3D Z_2 gauge theory (considered below), another limit is easier for MC simulations

$$n \rightarrow \infty, \quad m = 1 \quad (m = 1 \text{ limit}). \quad (5.14)$$

This new $m = 1$ limit can be also described by EST but one needs some care about the order counting for the one-loop power correction. This power correction is computed only for rectangles [19], [20] but the structure of this correction (order counting and scaling properties) is under control for any polygon.

In case of hexagons $H_{n,m}$ the transition from the one-loop EST expression for Wilson loops $W_{\text{EST}}^{1\text{-loop}}(H_{n,m})$ to the two-loop EST result $W_{\text{EST}}^{2\text{-loop}}(H_{n,m})$ is given by

$$W(H_{n,m}) = W_{\text{EST}}^{1\text{-loop}}(H_{n,m}) \left[1 + \frac{1}{n^2} f\left(\frac{m}{n}\right) + \dots \right]. \quad (5.15)$$

Here $f(x)$ is an unknown function. Within this two-loop accuracy we find from eq. (5.6)

$$r_{n,1} \stackrel{n \rightarrow \infty}{\equiv} r_{n,1}^{\text{EST1}} \frac{\sqrt{\left[1 + \frac{1}{n^2} f\left(\frac{1}{n}\right)\right] \left[1 + \frac{1}{n^2} f\left(-\frac{1}{n}\right)\right]}}{1 + \frac{1}{n^2} f(0)} \quad (5.16)$$

where

$$r_{n,1}^{\text{EST1}} = \left\{ \frac{\text{Det}[-\Delta_\zeta(H_{n,0})]}{\sqrt{\text{Det}[-\Delta_\zeta(H_{n,1})] \text{Det}[-\Delta_\zeta(H_{n,-1})]}} \right\}^{D-2}. \quad (5.17)$$

Here

$$\frac{\sqrt{\left[1 + \frac{1}{n^2} f\left(\frac{1}{n}\right)\right] \left[1 + \frac{1}{n^2} f\left(-\frac{1}{n}\right)\right]}}{1 + \frac{1}{n^2} f(0)} \stackrel{n \rightarrow \infty}{\equiv} 1 + \frac{1}{2n^4} f''(0) + O(n^{-6}). \quad (5.18)$$

Hence

$$r_{n,1} \stackrel{n \rightarrow \infty}{\equiv} r_{n,1}^{\text{EST1}} [1 + O(n^{-4})]. \quad (5.19)$$

A similar argument shows that

$$\frac{\text{Det}[-\Delta_\zeta(H_{n,0})]}{\sqrt{\text{Det}[-\Delta_\zeta(H_{n,1})] \text{Det}[-\Delta_\zeta(H_{n,-1})]}} = 1 + O(n^{-2}). \quad (5.20)$$

We see that in the $m = 1$ case EST predicts that

$$r_{n,1}^{\text{EST1}} \stackrel{n \rightarrow \infty}{\equiv} 1 + O(n^{-2}), \quad (5.21)$$

$$r_{n,1} \stackrel{n \rightarrow \infty}{\simeq} 1 + O(n^{-2}) , \quad (5.22)$$

$$\frac{r_{n,1}}{r_{n,1}^{\text{EST1}}} \stackrel{n \rightarrow \infty}{\simeq} 1 + O(n^{-4}) . \quad (5.23)$$

As a consequence,

$$\lim_{n \rightarrow \infty} \frac{|r_{n,1} - r_{n,1}^{\text{EST1}}|}{|r_{n,1}^{\text{EST1}} - 1|} = 0 . \quad (5.24)$$

Repeating the same arguments for ratios $q_{n,1}^\pm$ (5.5) and defining

$$(q_{n,1}^\pm)^{\text{EST1}} = e^{\sigma n} \left[\frac{\text{Det}[-\Delta_\zeta(H_{n,\pm 1})]}{\text{Det}[-\Delta_\zeta(H_{n,0})]} \right]^{\pm(D-2)/2} , \quad (5.25)$$

we arrive at

$$\frac{q_{n,1}^\pm}{(q_{n,1}^\pm)^{\text{EST1}}} \stackrel{n \rightarrow \infty}{\simeq} 1 + O(n^{-3}) , \quad (5.26)$$

$$e^{-\sigma n} (q_{n,1}^\pm)^{\text{EST1}} = 1 + O(n^{-2}) . \quad (5.27)$$

6 Comparison of lattice MC results with EST

6.1 Lattice parameters

Our lattice MC computation of Wilson loops $W(H_{n,m})$ for hexagons $H_{n,m}$ (5.2) in gauge theory \mathbb{Z}_2 was done in the dual Ising model at

$$\beta_I = 0.23 . \quad (6.1)$$

According to (3.7) this corresponds to \mathbb{Z}_2 coupling

$$\beta_{\mathbb{Z}_2} = 0.743543 . \quad (6.2)$$

These values of $\beta_{\mathbb{Z}_2}$ and β_I deviate from the critical point (3.11) and (3.12) towards the confinement phase of the \mathbb{Z}_2 gauge theory (which corresponds to the spontaneously broken phase of Ising model).

Our choice of values (3.11) and (3.12) for MC simulation is a compromise between two constraints:

- continuous limit $\beta_{\mathbb{Z}_2} \rightarrow \beta_{\mathbb{Z}_2}^{\text{crit}}$,
- large-size limit of Wilson contours C .

From the formal theoretical point of view, the continuous limit $\beta_{\mathbb{Z}_2} \rightarrow \beta_{\mathbb{Z}_2}^{\text{crit}}$ must be taken first and only after that one can study the asymptotic large-size expansion of Wilson loops. In practical MC simulations the choice of relevant values of β and loop-sizes for the comparison of EST is a subtle problem. Our choice of β_I value (6.1) is motivated by several factors:

1) Agreement of other MC simulations using β_I value (6.1) and “worse” values of β_I with EST, see e.g. ref. [15].

Size parameter n of hexagon $H_{n,m}$	8	16	24	32
Lattice size	96^3	96^3	120^3	180^3

Table 1: 3D lattice sizes used for the MC computation of ratios of hexagon Wilson loops $W(H_{n,m})$.

2) In case of the large-size limit for polygonal Wilson loops the accuracy of EST is controlled by the size of single sides of the polygon and not by the overall size of the polygon. Hence one has to work with rather large polygons. Therefore it makes sense to sacrifice the “quality” of β_I and to invest computer resources in the computation of larger Wilson loops.

3) String tension σ of the \mathbb{Z}_2 model (coinciding with the surface tension of Ising model) at point β_I (6.1), is known with a high precision [15]:

$$\sigma = 0.0228068(15). \quad (6.3)$$

This high-precision value of σ is used in our comparison of MC results with EST in sec. 6.4.

We compute Wilson loops for polygons $H_{n,m}$ (5.2) with

$$m = 0, \pm 1 \quad (6.4)$$

in the large n limit. The following values of n were used in our MC computation:

$$n = 8, 16, 24, 32. \quad (6.5)$$

Lattice sizes used in the MC computation of Wilson loops $W(H_{n,m})$ are listed in Table 1.

The technical implementation of MC simulations uses standard optimization methods which are well described in literature [20], [68]. The HMC algorithm (sec. 3.2.5) is crucial for reaching a rather high accuracy of MC results.

6.2 Two methods for the analysis of lattice MC data

One can compare lattice MC results with EST for large Wilson loops using two methods. Method 1 deals with universal predictions of EST which are formulated in terms of ratios of Wilson loops $r_{n,1}$ (5.6) without using string tension σ . Method 2 uses high-precision value of string tension (6.3) and deals with quantities $q_{n,1}^\pm$ (5.5) involving both ratios of Wilson loops and string tension σ .

An advantage of method 1 is its simplicity which allows for a fast but incomplete comparison of lattice MC results with EST predictions. Ratios $r_{n,1}$ used in method 1 have a universal large-size one-loop asymptotic behavior independent of the gauge group. However,

1) $q_{n,1}^\pm$ are primary MC computed quantities, ratios $r_{n,1}$ are computed via MC results for $q_{n,1}^\pm$ using eq. (5.6).

2) EST provides predictions not only for $r_{n,1}$ but also for $q_{n,1}^\pm$ (if one knows string tension σ from external MC results).

3) When one computes $r_{n,1}$ via $q_{n,1}^\pm$ (5.6), one has a certain information loss. Indeed, according to (5.25) – (5.27) at large n

$$|q_{n,1}^+ - q_{n,1}^-| \ll |1 - q_{n,1}^\pm| \quad (6.6)$$

so that in ratio $r_{n,1} = q_{n,1}^-/q_{n,1}^+$

- significant information cancels,
- statistical errors increase.

To summarize, method 1 is simple and transparent but incomplete in comparison with more thorough method 2.

6.3 Method 1: universal predictions of EST

Method 1 is based on ratios of Wilson loops $r_{n,1}$. Theoretically ratios $r_{n,1}$ are defined by eq. (5.6)

$$r_{n,1} = \frac{W(H_{n,-1})W(H_{n,1})}{[W(H_{n,0})]^2}. \quad (6.7)$$

Here $W(H_{n,m})$ is Wilson loop for hexagon $H_{n,m}$ whose geometry is given by eq. (5.2), see Fig. 1b. We use notation $r_{n,1}^{\text{MC}}$ for lattice MC data and $r_{n,1}^{\text{EST1}}$ for one-loop EST results. In lattice MC computation in Ising model based on HMC algorithm (see sec. 3.2.5), MC values $r_{n,1}^{\text{MC}}$ are computed using decomposition

$$r_{n,1}^{\text{MC}} = \frac{(q_{n,1}^-)^{\text{MC}}}{(q_{n,1}^+)^{\text{MC}}}, \quad (6.8)$$

$$(q_{n,1}^-)^{\text{MC}} = \left[\frac{W(H_{n,-1})}{W(H_{n,0})} \right]^{\text{MC}}, \quad (6.9)$$

$$(q_{n,1}^+)^{\text{MC}} = \left[\frac{W(H_{n,0})}{W(H_{n,1})} \right]^{\text{MC}}. \quad (6.10)$$

In HMC method ratios $(q_{n,1}^\pm)^{\text{MC}}$ are computed directly without computing single Wilson loops $W(H_{n,m})$. The resulting values $r_{n,1}^{\text{MC}}$ are listed in Table 2. The underlying values of $(q_{n,1}^\pm)^{\text{MC}}$ can be found in Table 3.

The one-loop EST prediction for $r_{n,1}$ is given by eq. (5.17) taken at $D = 3$

$$r_{n,1}^{\text{EST1}} = \frac{\text{Det}[-\Delta_\zeta(H_{n,0})]}{\sqrt{\text{Det}[-\Delta_\zeta(H_{n,1})]\text{Det}[-\Delta_\zeta(H_{n,-1})]}}. \quad (6.11)$$

Table 2 lists numerical values of $r_{n,1}^{\text{EST1}}$ computed using numerical values Laplace determinants from Table 4.

In order to check the agreement of EST ratios $r_{n,1}^{\text{EST1}}$ with corresponding lattice MC ratios $r_{n,1}^{\text{MC}}$, one should keep in mind the accuracy of EST asymptotic

n	$r_{n,1}^{\text{EST1}}$	$r_{n,1}^{\text{MC}}$	$\frac{r_{n,1}^{\text{MC}}}{r_{n,1}^{\text{EST1}}} - 1$	$\frac{r_{n,1}^{\text{MC}} - r_{n,1}^{\text{EST1}}}{r_{n,1}^{\text{EST1}} - 1}$	$d(n)$
8	1.00312545	1.001703(13)	-0.001418(13)	-0.455(4)	5.808(53)
16	1.00076881	1.0006323(55)	-0.0001364(55)	-0.1776(72)	8.94(36)
24	1.00034068	1.0003190(44)	-0.0000216(44)	-0.063(13)	7.2 ± 1.5
32	1.00019143	1.000196(18)	0.000004(18)	0.023(92)	-5 ± 19

Table 2: Comparison of lattice MC results for triple hexagon Wilson loop ratios $r_{n,1}^{\text{MC}}$ with EST asymptotic expression $r_{n,1}^{\text{EST1}}$.

formulas (5.21) – (5.24). The data presented in Table 2 definitely agree with the main prediction of EST (5.24)

$$\lim_{n \rightarrow \infty} \frac{|r_{n,1} - r_{n,1}^{\text{EST1}}|}{|r_{n,1}^{\text{EST1}} - 1|} = 0. \quad (6.12)$$

However, the confirmation of the more subtle limit testing the scaling of the two-loop EST correction (5.23)

$$d(n) = n^4 \left(1 - \frac{r_{n,1}^{\text{MC}}}{r_{n,1}^{\text{EST1}}} \right), \quad (6.13)$$

$$\lim_{n \rightarrow \infty} d(n) = \text{finite} \neq 0 \quad (6.14)$$

is less reliable because

1) at $n = 8$ asymptotic formulas of EST may have large contributions from higher orders,

2) at $n = 32$ the MC data have a too large statistical error.

Therefore one gets a confirmation for scaling (6.14) of the two-loop EST correction only from the agreement of $n = 16$ and $n = 24$ values for $n^4 (r_{n,1}/r_{n,1}^{\text{EST1}} - 1)$.

6.4 Method 2: analysis using the value of the string tension

Method 2 is based on quantities $q_{n,1}^{\pm}$ which are defined by eq. (5.5)

$$q_{n,1}^{\pm} = \left[\frac{W(H_{n,0})}{W(H_{n,\pm 1})} \right]^{\pm 1}. \quad (6.15)$$

EST predictions for these ratios are described by eqs. (5.25) – (5.27). We introduce notation:

$$(q_{n,1}^+)^{\text{EST0}} = (q_{n,1}^-)^{\text{EST0}} = e^{\sigma n}. \quad (6.16)$$

n	α	$(q_{n,1}^\alpha)^{\text{EST0}}$	$(q_{n,1}^\alpha)^{\text{EST1}}$	$(q_{n,1}^\alpha)^{\text{MC}}$	$\frac{(q_{n,1}^\alpha)^{\text{MC}}}{(q_{n,1}^\alpha)^{\text{EST1}}} - 1$
8	-	1.200159(14)	1.221022(15)	1.221009(11)	-0.000011(15)
8	+	1.200159(14)	1.217218(15)	1.218933(11)	0.001409(15)
16	-	1.440383(35)	1.452138(35)	1.4521592(55)	0.000014(24)
16	+	1.440383(35)	1.451023(35)	1.4512416(58)	0.000151(24)
24	-	1.728689(62)	1.737913(63)	1.7376523(52)	-0.000150(36)
24	+	1.728689(62)	1.737321(63)	1.7370981(56)	-0.000128(36)
32	-	2.07470(10)	2.08293(10)	2.082510(27)	-0.000200(50)
32	+	2.07470(10)	2.08253(10)	2.082102(25)	-0.000204(49)

Table 3: Comparison of lattice MC results for double ratios $(q_{n,1}^\pm)^{\text{MC}}$ of hexagon Wilson loops with EST asymptotic leading-order values $(q_{n,1}^\alpha)^{\text{EST0}}$ and with one-loop results $(q_{n,1}^\alpha)^{\text{EST1}}$.

We use the value of string tension σ (6.3). Quantities $(q_{n,1}^\pm)^{\text{EST1}}$ are defined by eq. (5.25). According to (5.26)

$$\frac{q_{n,1}^\pm}{(q_{n,1}^\pm)^{\text{EST1}}} - 1 \stackrel{n \rightarrow \infty}{\simeq} O(n^{-3}). \quad (6.17)$$

In Table 3 we list

- 1) lattice MC results for $(q_{n,1}^\pm)^{\text{MC}}$,
- 2) values for quantity $(q_{n,1}^\pm)^{\text{EST0}}$ (6.16) using the value of string tension σ (6.3),
- 3) values for $(q_{n,1}^\pm)^{\text{EST1}}$ (5.25) computed using σ (6.3) and Laplace determinants listed in Table 4.

The data presented in Table 3 show a fast decay of

$$\frac{(q_{n,1}^\alpha)^{\text{MC}}}{(q_{n,1}^\alpha)^{\text{EST1}}} - 1 \quad (6.18)$$

at large n . For all values $n = 8, 16, 24, 32$ we have

$$\left| \frac{(q_n^\alpha)^{\text{EST1}} - (q_n^\alpha)^{\text{MC}}}{(q_n^\alpha)^{\text{EST0}} - (q_n^\alpha)^{\text{MC}}} \right| \ll 1.$$

However, the $O(n^{-3})$ behavior of EST prediction (6.17) cannot be confirmed because of the insufficient accuracy of lattice MC results for $n = 24$ and $n = 32$.

7 Conclusions

To summarize, our lattice MC results for large hexagon Wilson loops are in a perfect agreement with EST. The achieved accuracy of MC simulations is sufficient to confirm the one-loop contribution of the Laplace determinants. The situation is less reliable for the two-loop correction. In the absence of the full theoretical expression for this correction we could test only its asymptotic scaling behavior which agrees with MC results but the accuracy of this test is not sufficient for making final decisive conclusions.

Acknowledgments

My gratitude comes late to my senior friends who passed away: W. Bathelt, D.I. Diakonov, K. Goeke, M. I. Polykarpov and N. G. Uraltsev. I am grateful for discussions and for a support to E. T. Akhmedov, A. A. Andrianov, E. N. Antonov, N. V. Antonov, G. S. Danilov, P. Druck, M. I. Eides, E. Epelbaum, N. Gromov, H. Dorn, V. A. Kudryavtsev, L. N. Lipatov, A. S. Losev, A. D. Mirlin, M. V. Polyakov, N. G. Stefanis, T. Takayanagi, S. I. Troyan, A. V. Yung and many others. This work would not be possible without the help of V. Yu. Petrov. The MC simulations at Theoretical Physics Division of Petersburg Nuclear Physics Institute were supported by Russian Science Foundation grant 14-22-00281. I also appreciate the possibility to use computer facilities provided by Institute for Theoretical Physics II of Ruhr University Bochum.

Appendix. Computation of Laplace determinants

A.1 2D Laplace determinant for general polygons

A.1.1 Result of Aurell and Salomonson

In this appendix we compute Laplace determinants for hexagons $H_{n,m}$ (5.2) using the general results of ref. [51]. In order to simplify the access to equations of ref. [51], in this appendix we try to be close to the original notation of ref. [51] (sometimes deviating from the notation used in the main part of this paper).

In ref. [51] interior vertex angles θ_ν of polygon P are parametrized by parameters β_ν

$$\theta_\nu = \pi(1 - \beta_\nu) , \tag{A.1}$$

$$0 < \beta_\nu < 1 , \tag{A.2}$$

$$1 \leq \nu \leq M . \tag{A.3}$$

Sum rule (2.16) for the angles takes the form

$$\sum_{\nu=1}^M \beta_\nu = 2 . \tag{A.4}$$

Eq. (55) of ref. [51] defines Schwarz-Christoffel (SC) mapping of the unit circle $|u| \leq 1$ in complex u -plane to polygon P in the z -plane

$$\frac{dz}{du} = e^{\lambda_0} \prod_{\nu=1}^M (u - e^{i\phi_\nu})^{-\beta_\nu} . \quad (\text{A.5})$$

Here $e^{i\phi_\nu}$ are points on the boundary of the unit circle which are mapped to vertices z_ν of polygon P . λ_0 is a real constant controlling the size of the polygon.

The general result for the determinant of Laplace operator defined in polygon P with Dirichlet boundary conditions in ζ -regularization (4.7) – (4.9) is given by eq. (62) of ref. [51]:

$$\begin{aligned} -\ln \text{Det}_\zeta [-\Delta(P)] &= \sum_{\mu=1}^M Z'_{1-\beta_\mu}(0) + \frac{\lambda_0}{12} \sum_{\mu=1}^M \frac{(2-\beta_\mu)\beta_\mu}{1-\beta_\mu} \\ &\quad - \frac{1}{12} \sum_{1 \leq \mu \neq \nu \leq M} \frac{\beta_\mu \beta_\nu}{1-\beta_\mu} \ln |(e^{i\phi_\mu} - e^{i\phi_\nu})| \end{aligned} \quad (\text{A.6})$$

where $Z'_\alpha(0)$ is the original notation of ref. [51] for a certain function of parameter α (so that $Z'_{1-\beta_\mu}(0)$ should be understood as the value of this function at $\alpha = 1 - \beta_\mu$). This function is defined by eqs. (51) – (54) of ref. [51] and is discussed below in sec. A.1.3 of this paper.

The λ_0 -dependent part on the RHS of eq. (A.6)

$$\frac{\lambda_0}{12} \sum_{\mu=1}^M \frac{(2-\beta_\mu)\beta_\mu}{1-\beta_\mu} = \frac{\lambda_0}{12} \sum_{\mu=1}^M \frac{\pi^2 - \theta_\mu^2}{\pi\theta_\mu} \quad (\text{A.7})$$

controls the dependence of the Laplace determinant on the size of the polygon and is in agreement with the scaling rule (4.3), (4.4), (4.10) for Laplace determinants.

A.1.2 SC mapping in semiplane parametrization

Paper [51] uses SC mapping (A.5) of the unit circle to the polygon. One can map unit circle in the u -plane to the upper semiplane of complex variable ω using linear-fractional transformation

$$\omega = i \frac{1-u}{1+u} \quad (\text{A.8})$$

with the inverse transformation

$$u = \frac{1+i\omega}{1-i\omega} . \quad (\text{A.9})$$

This maps points $e^{i\phi_\nu}$ on the boundary of the unit circle in the u -plane to points ω_ν on the real axis of the ω -plane

$$\omega_\nu = \tan\left(\frac{1}{2}\phi_\nu\right) , \quad (\text{A.10})$$

$$e^{i\phi_\nu} = \frac{1 + i\omega_\nu}{1 - i\omega_\nu}. \quad (\text{A.11})$$

Defining

$$\chi_P = \frac{1}{2}e^{\lambda_0} \left[-i \exp \left(\frac{i}{2} \sum_{\mu=1}^M \beta_\mu \phi_\mu \right) \right] \left[\prod_{\mu=1}^M \left[\cos \left(\frac{1}{2} \phi_\mu \right) \right]^{-\beta_\mu} \right], \quad (\text{A.12})$$

one finds that in terms of the ω -plane parametrization, SC transformation (A.5) becomes

$$\frac{dz}{d\omega} = \chi_P \prod_{\nu=1}^M (\omega - \omega_\nu)^{-\beta_\nu}. \quad (\text{A.13})$$

The upper semiplane

$$\text{Im } \omega \geq 0 \quad (\text{A.14})$$

is mapped to the polygon in the complex z -plane. Points ω_ν on the real axis of the ω plane are mapped to vertices z_ν of the polygon in the z plane. The side lengths $|z_{\mu+1} - z_\mu|$ of the polygon are given by integrals

$$|z_{\mu+1} - z_\mu| = |\chi_P| \int_{\omega_\mu}^{\omega_{\mu+1}} d\omega \prod_{\nu=1}^M |\omega - \omega_\nu|^{-\beta_\nu}. \quad (\text{A.15})$$

In terms of this semiplane version of SC transformation, Laplace determinant (A.6) becomes

$$\ln \text{Det}_\zeta [-\Delta(P)] = \{\ln \text{Det}_\zeta [-\Delta(P)]\}^{(1)} + \{\ln \text{Det}_\zeta [-\Delta(P)]\}^{(2)} \quad (\text{A.16})$$

where

$$\{\ln \text{Det}_\zeta [-\Delta(P)]\}^{(1)} = \frac{1}{12} \sum_{1 \leq \mu \neq \nu \leq M} \frac{\beta_\mu \beta_\nu}{1 - \beta_\mu} \ln \left| \frac{\omega_\mu - \omega_\nu}{\chi_P} \right|, \quad (\text{A.17})$$

$$\{\ln \text{Det}_\zeta [-\Delta(P)]\}^{(2)} = - \sum_{\mu=1}^M Z'_{1-\beta_\mu}(0). \quad (\text{A.18})$$

A.1.3 Contribution $\{\ln \text{Det}_\zeta [-\Delta(P)]\}^{(2)}$

Contribution $\{\ln \text{Det}_\zeta [-\Delta(P)]\}^{(2)}$ (A.18) depends only on the angles of the polygon and is additive. Therefore this contribution cancels in any combinations of Wilson loops obeying vertex balance condition (1.9). From this point of view, term $\{\ln \text{Det}_\zeta [-\Delta(P)]\}^{(2)}$ is irrelevant for our *final* aims. On the other hand, our *intermediate* results deal with single Laplace determinants. In particular, numerical values listed for Laplace determinants in Table 4 contain the contribution $\{\ln \text{Det}_\zeta [-\Delta(P)]\}^{(2)}$ (A.18) which depends on function $Z'_\alpha(0)$.

The computation of function $Z'_\alpha(0)$ is an essential part of ref. [51]. However, in lattice applications one usually deals with polygons containing only angles $\pi/2$ and $3\pi/2$ corresponding to $\beta_\mu = \pm 1/2$ so that one needs only the values for $Z'_{1/2}(0)$ and $Z'_{3/2}(0)$. Function $Z'_\alpha(0)$ is a smooth function of parameter α in the range $-1 < \alpha < 1$ which allows for an integral representation. The integral can be computed analytically when α is rational, i.e. $\alpha = p/q$ where p, q are integer. According to eqs. (102), (103) of ref. [51]

$$Z'_{1/q}(0) = \frac{q-1}{4q} \ln \pi - \left(\frac{q}{12} - \frac{1}{4} + \frac{1}{6q} \right) \ln 2 + \left(\frac{1}{4} - \frac{1}{12q} \right) \ln q + \sum_{s=1}^{q-1} \left(\frac{1}{2} - \frac{s}{q} \right) \ln \Gamma \left(\frac{s}{q} \right), \quad (\text{A.19})$$

$$Z'_{p/q}(0) = \frac{q-p}{4q} \ln(2\pi) + \frac{p^2 - q^2}{12pq} \ln 2 - \frac{1}{q} \left(p - \frac{1}{p} \right) \zeta'(-1) - \frac{1}{12pq} \ln q + \left[\frac{1}{4} + S(q, p) \right] \ln \frac{q}{p} + \sum_{r=1}^{p-1} \left(\frac{1}{2} - \frac{r}{p} \right) \ln \Gamma \left(\frac{R(rq, p)}{p} \right) + \sum_{s=1}^{q-1} \left(\frac{1}{2} - \frac{s}{q} \right) \ln \Gamma \left(\frac{R(sp, q)}{q} \right). \quad (\text{A.20})$$

Here ζ' is the derivative of Riemann ζ function:

$$\zeta(z) = \sum_{n=1}^{\infty} n^{-z}, \quad (\text{A.21})$$

$$\zeta'(z) = \frac{d\zeta(z)}{dz}. \quad (\text{A.22})$$

$S(q, p)$ is Dedekind sum:

$$S(q, p) = \frac{1}{p} \sum_{r=0}^{p-1} r \left[\frac{R(rq, p)}{p} - \frac{1}{2} \right] \quad (\text{A.23})$$

where $R(n, p)$ is the non-negative remainder of the division of n by p :

$$n = pm + R(n, p), \quad 0 \leq R(n, p) \leq p - 1. \quad (\text{A.24})$$

Keep in mind that the definition of Dedekind sum given in eq. (98) of article [51] has a typo: one should replace $S(p, q)$ by $S(q, p)$ on the LHS of *that* equation like it is done in eq. (A.23) of *this* article. After this correction one easily derives from eq. (A.19)

$$Z'_{1/2}(0) = \frac{1}{8} \ln(2\pi) + \frac{1}{12} \ln 2 \quad (\text{A.25})$$

and from eq. (A.20)

$$Z'_{3/2}(0) = -\frac{1}{8} \ln\left(\frac{\pi}{2}\right) - \frac{7}{36} \ln 3 - \frac{4}{3} \zeta'(-1) + \frac{1}{6} \ln \frac{\Gamma(2/3)}{\Gamma(1/3)} \quad (\text{A.26})$$

A lattice polygon with M vertices contains $(M-4)/2$ vertices with angle $3\pi/2$ and $(M+4)/2$ vertices with angle $\pi/2$ so that for this class of polygons we find from eq. (A.18)

$$\begin{aligned} \{\ln \text{Det}_\zeta [-\Delta(P)]\}^{(2)} &= -\left(\frac{M+4}{2}\right) Z'_{1/2}(0) - \left(\frac{M-4}{2}\right) Z'_{3/2}(0) \\ &= -\left(\frac{M+4}{2}\right) \left[\frac{1}{8} \ln(2\pi) + \frac{1}{12} \ln 2\right] \\ &\quad - \left(\frac{M-4}{2}\right) \left[-\frac{1}{8} \ln\left(\frac{\pi}{2}\right) - \frac{7}{36} \ln 3 - \frac{4}{3} \zeta'(-1) + \frac{1}{6} \ln \frac{\Gamma(2/3)}{\Gamma(1/3)}\right]. \end{aligned} \quad (\text{A.27})$$

In case of a hexagon with $M = 6$ this reduces to

$$\{\ln \text{Det}_\zeta [-\Delta(P)]\}^{(2)} = -\frac{1}{2} \ln \pi - \frac{7}{6} \ln 2 + \frac{7}{36} \ln 3 + \frac{4}{3} \zeta'(-1) - \frac{1}{6} \ln \frac{\Gamma(2/3)}{\Gamma(1/3)}. \quad (\text{A.28})$$

A.1.4 Contribution $\{\ln \text{Det}_\zeta [-\Delta(P)]\}^{(1)}$

The rest of the problem is the computation of $\{\ln \text{Det}_\zeta [-\Delta(P)]\}^{(1)}$ (A.17). This computation consists of two parts:

1) For a given polygon with vertices given by complex plane coordinates z_μ , solve SC eq. (A.15) and find real parameters ω_μ and (generally complex) parameter χ_P . This inverse problem has many solutions because of the freedom of real linear fractional transformations mapping the upper semiplane of complex ω to itself.

2) Using solution $\{\omega_\mu\}$, one can compute the RHS of expression (A.17) for $\{\ln \text{Det}_\zeta [-\Delta(P)]\}^{(1)}$, the result is invariant with respect to real linear fractional transformations of $\{\omega_\mu\}$.

Generally, equation (A.15) for $\{\omega_\mu\}$ can be solved only numerically. But in the case of hexagon $H_{n,0}$ (5.2) the integrals on the RHS of eq. (A.15) can be expressed via the hypergeometric function.

A.2 Case of symmetric hexagon

A.2.1 Hexagon P_{ab}

Let us consider hexagon P_{ab} with parametrization (5.1)

$$P_{ab} = P\left(a+b, \frac{\pi}{2}, a+b, \frac{\pi}{2}, a, \frac{\pi}{2}, b, \frac{3\pi}{2}, b, \frac{\pi}{2}, a, \frac{\pi}{2}\right). \quad (\text{A.29})$$

In case $a = b = n$ this hexagon coincides with hexagon $H_{n,0}$ defined by eq. (5.2) and used in our MC computation:

$$P_{nn} = H_{n,0}. \quad (\text{A.30})$$

But in case $a \neq b$ hexagons P_{ab} are different from hexagons $H_{n,0}$ (5.2). Hexagons P_{ab} are distinguished by the reflection symmetry with respect to the diagonal axis passing through $3\pi/2$ vertex of this polygon. It is well known that combining reflection symmetries of polygons with Schwarz symmetry principle, one can simplify SC integrals. In particular, the reflection symmetry of hexagons P_{ab} allows to express SC integral (A.15) via the hypergeometric function. Below we compute Laplace determinant for the polygon P_{ab} for the general case $a \neq b$ although for the comparison of our lattice MC results with EST

- 1) only the case $a = b$ is relevant,
- 2) we also need Laplace determinants for polygons $H_{n,\pm 1}$ which cannot be reduced to the hypergeometric function.

A.2.2 Inverse SC problem for hexagon P_{ab}

Using the diagonal reflection symmetry of hexagon P_{ab} , we can choose parameters ω_μ in the following way

$$\omega_1 < \omega_2 < \omega_3 < \omega_4 < \omega_5, \quad (\text{A.31})$$

$$\omega_3 = 0, \quad (\text{A.32})$$

$$-\omega_2 = \omega_4 = 1, \quad (\text{A.33})$$

$$-\omega_1 = \omega_5 = w > 1, \quad (\text{A.34})$$

$$\omega_6 \rightarrow \infty. \quad (\text{A.35})$$

We choose ω_6 to be SC mapped to the $3\pi/2$ vertex of the polygon. Then angular parameters β_μ (A.1) of our hexagon P_{ab} are

$$\beta_1 = \beta_2 = \beta_3 = \beta_4 = \beta_5 = -\beta_6 = \frac{1}{2}. \quad (\text{A.36})$$

In order to keep the size of the polygon fixed in the limit $\omega_6 \rightarrow \infty$, we must take the limit

$$\chi_P \rightarrow 0 \quad (\text{A.37})$$

for parameter χ_P in eq. (A.13) and keep the combination

$$\chi_P |\omega_6|^{1/2} \equiv \psi_P = \text{const} \quad (\text{A.38})$$

fixed in the limit $\omega_6 \rightarrow \infty$.

Then SC equations (A.15) reduce to

$$|\psi_P| \int_0^1 d\omega f(\omega) = a + b, \quad (\text{A.39})$$

$$|\psi_P| \int_1^w d\omega f(\omega) = a, \quad (\text{A.40})$$

$$|\psi_P| \int_w^\infty d\omega f(\omega) = b, \quad (\text{A.41})$$

where

$$f(\omega) = |\omega(\omega^2 - w^2)(\omega^2 - 1)|^{-1/2}. \quad (\text{A.42})$$

We find from eqs. (A.39), (A.41)

$$\frac{a+b}{b} = \frac{\int_0^1 d\omega f(\omega)}{\int_w^\infty d\omega f(\omega)}. \quad (\text{A.43})$$

These integrals can be expressed via the hypergeometric function $F(\alpha, \beta, \gamma, z)$:

$$F(\alpha, \beta, \gamma, z) = \sum_{n=0}^{\infty} \frac{(\alpha)_n (\beta)_n}{(\gamma)_n n!} z^n, \quad (\text{A.44})$$

$$(\alpha)_n = \frac{\Gamma(\alpha + n)}{\Gamma(\alpha)}, \quad (\text{A.45})$$

$$I_1 = \int_0^1 d\omega f(\omega) = \frac{1}{2w\sqrt{2\pi}} \left[\Gamma\left(\frac{1}{4}\right) \right]^2 F\left(\frac{1}{4}, \frac{1}{2}, \frac{3}{4}, w^{-2}\right), \quad (\text{A.46})$$

$$I_2 = \int_w^\infty d\omega f(\omega) = \left(\frac{2\pi}{w}\right)^{3/2} \left[\Gamma\left(\frac{1}{4}\right) \right]^{-2} F\left(\frac{3}{4}, \frac{1}{2}, \frac{5}{4}, w^{-2}\right). \quad (\text{A.47})$$

Now eq. (A.43) gives

$$\frac{a+b}{b} = \frac{1}{8\pi^2} \left[\Gamma\left(\frac{1}{4}\right) \right]^4 w^{1/2} \frac{F\left(\frac{1}{4}, \frac{1}{2}, \frac{3}{4}, w^{-2}\right)}{F\left(\frac{3}{4}, \frac{1}{2}, \frac{5}{4}, w^{-2}\right)}. \quad (\text{A.48})$$

For given geometrical parameters a, b of hexagon P_{ab} , eq. (A.48) determines parameter $w > 1$ which in turn controls SC parameters $-\omega_1 = \omega_5 = w$ (A.34). Thus we have reduced the inverse SC problem (A.15) of expressing SC parameters ω_k via geometrical parameters z_k to eq. (A.48).

A.2.3 Laplace determinant for hexagon P_{ab}

In case of

- hexagons with angular parameters β_μ (A.36),
- SC parameter ω_6 taken to infinity

the sum on the RHS of eq. (A.17) becomes

$$\begin{aligned}
& 2 \sum_{1 \leq \mu \neq \nu \leq 6} \frac{\beta_\mu \beta_\nu}{1 - \beta_\mu} \ln \left| \frac{\omega_\mu - \omega_\nu}{\chi_P} \right| \\
&= \sum_{1 \leq \mu \neq \nu \leq 5} \ln \left| \frac{\omega_\mu - \omega_\nu}{\chi_P} \right| - \sum_{1 \leq \mu \leq 5} \ln \left| \frac{\omega_\mu - \omega_6}{\chi_P} \right| - \frac{1}{3} \sum_{1 \leq \nu \leq 5} \ln \left| \frac{\omega_\nu - \omega_6}{\chi_P} \right| \\
&\xrightarrow{\omega_6 \rightarrow 0} \sum_{1 \leq \mu \neq \nu \leq 5} \ln |\omega_\mu - \omega_\nu| - \frac{20}{3} \ln |\omega_6 \chi_P^2| . \tag{A.49}
\end{aligned}$$

Combining this with (A.38), we find

$$2 \sum_{1 \leq \mu \neq \nu \leq 6} \frac{\beta_\mu \beta_\nu}{1 - \beta_\mu} \ln \left| \frac{\omega_\mu - \omega_\nu}{\chi_P} \right| = \sum_{1 \leq \mu \neq \nu \leq 5} \ln |\omega_\mu - \omega_\nu| - \frac{40}{3} \ln |\psi_P| . \tag{A.50}$$

In case of hexagon P_{ab} with parameters ω_μ (A.32) – (A.35) we have

$$\sum_{1 \leq \mu \neq \nu \leq 5} \ln |\omega_\mu - \omega_\nu| = \ln \left| 4w^3 (w^2 - 1)^2 \right| .$$

Now we insert these results into eq. (A.17)

$$[\ln \text{Det}_\zeta (-\Delta (P_{ab}))]^{(1)} = \frac{1}{6} \ln \left| 2w^{3/2} (w^2 - 1) \right| - \frac{5}{9} \ln (|\psi_P|) . \tag{A.51}$$

According to eq. (A.39)

$$\psi_P = \frac{a + b}{I_1} \tag{A.52}$$

so that

$$[\ln \text{Det}_\zeta (-\Delta (P_{ab}))]^{(1)} = -\frac{5}{9} \ln (a + b) + \frac{1}{6} \ln \left| 2w^{3/2} (w^2 - 1) \right| + \frac{5}{9} \ln I_1 . \tag{A.53}$$

Inserting this result with I_1 given by (A.46) into eq. (A.16) and using expression (A.28) for $\{\ln \text{Det}_\zeta [-\Delta (P)]\}^{(2)}$, we find

$$\begin{aligned}
\ln \text{Det}_\zeta [-\Delta (P_{ab})] &= -\frac{5}{9} \ln (a + b) \tag{A.54} \\
&- \frac{1}{2} \ln \pi - \frac{7}{6} \ln 2 + \frac{7}{36} \ln 3 + \frac{4}{3} \zeta'(-1) - \frac{1}{6} \ln \frac{\Gamma(2/3)}{\Gamma(1/3)} \\
&+ \frac{1}{6} \ln \left| 2w^{3/2} (w^2 - 1) \right| + \frac{5}{9} \ln \left\{ \frac{1}{2\sqrt{2\pi}w} \left[\Gamma\left(\frac{1}{4}\right) \right]^2 F\left(\frac{1}{4}, \frac{1}{2}, \frac{3}{4}, w^{-2}\right) \right\} . \tag{A.55}
\end{aligned}$$

This result, taken together with eq. (A.48) defining parameter w , solves the problem of the Laplace determinant for symmetric hexagon P_{ab} (A.29).

A.2.4 Laplace determinant for hexagon $H_{n,0}$

Setting

$$a = b = n \quad (\text{A.56})$$

in eq. (A.55) and using eq. (A.30), we find

$$\begin{aligned} \ln \text{Det}_\zeta [-\Delta (H_{n,0})] &= -\frac{5}{9} \ln n \\ &+ \frac{1}{18} (-46 \ln 2 + 5 \ln 3 - 17 \ln \pi) + \frac{4}{3} \zeta'(-1) + \frac{1}{3} \ln \Gamma\left(\frac{1}{3}\right) \\ &- \frac{11}{36} \ln w_0 + \frac{1}{6} \ln (w_0^2 - 1) + \frac{5}{9} \ln \left\{ \left[\Gamma\left(\frac{1}{4}\right) \right]^2 F\left(\frac{1}{4}, \frac{1}{2}, \frac{3}{4}, w_0^{-2}\right) \right\} \end{aligned} \quad (\text{A.57})$$

where $w_0 > 1$ is the solution of equation (A.48) with $a = b$

$$\frac{1}{16\pi^2} \left[\Gamma\left(\frac{1}{4}\right) \right]^4 w_0^{1/2} \frac{F\left(\frac{1}{4}, \frac{1}{2}, \frac{3}{4}, w_0^{-2}\right)}{F\left(\frac{3}{4}, \frac{1}{2}, \frac{5}{4}, w_0^{-2}\right)} = 1. \quad (\text{A.58})$$

The numerical solution of eq. (A.58) is

$$w_0 = 1.154700538379251529018297561 \dots \quad (\text{A.59})$$

Now eq. (A.57) gives

$$\ln \text{Det}_\zeta [-\Delta (H_{1,0})] = -1.11547761205543217467 \dots \quad (\text{A.60})$$

Using eq. (A.57), one can rederive relation (5.12) expressing $\ln \text{Det}_\zeta [-\Delta (H_{n,0})]$ via $\ln \text{Det}_\zeta [-\Delta (H_{1,0})]$.

A.3 Numerical results for Laplace determinants

In case of polygons $H_{n,\pm 1}$, SC integrals (A.15) can be reduced (after taking the limit $\omega_6 \rightarrow \infty$) to integrals of type

$$\int_{\omega_i}^{\omega_j} d\omega \left[\prod_{k=1}^5 (\omega - \omega_k) \right]^{-1/2}. \quad (\text{A.61})$$

The computation of Laplace determinants for $H_{n,\pm 1}$ repeats the same steps as in the case of $H_{n,0} = P_{nn}$ considered above but now one has to combine

- the computation of SC integrals (A.15),
- the solution of equations (A.15) with respect to ω_k

in one numerical bundle. One can recommend book [79] and software packages developed by its authors: SCPACK (Fortran, L.N. Trefethen) [80] and SC Toolbox (MATLAB, T.A. Driscoll) [81]. Although a straightforward numerical approach is not a problem for simple polygons like our hexagons $H_{n,m}$, these packages (in principle, designed for more complicated polygons) may be helpful.

n	$\ln \text{Det}_\zeta [-\Delta (H_{n,-1})]$	$\ln \text{Det}_\zeta [-\Delta (H_{n,0})]$	$\ln \text{Det}_\zeta [-\Delta (H_{n,1})]$
8	-2.30519045940400	-2.27072291298867	-2.24249651205329
16	-2.67206125015434	-2.65580467996642	-2.64108514509615
24	-2.89170650424248	-2.88106307335984	-2.87110088157089
32	-3.04879906577170	-3.04088644694416	-3.03335665452480

Table 4: Numerical results for logarithms of Laplace determinants $\text{Det}_\zeta [-\Delta (H_{n,m})]$ in ζ -regularization for hexagon regions $H_{n,m}$ with Dirichlet boundary condition.

Our final numerical results for all Laplace determinants needed for the comparison of our lattice MC results with EST, i.e. for $\text{Det}_\zeta [-\Delta (H_{n,m})]$ with

$$n = 8, 16, 24, 32, \quad (\text{A.62})$$

$$m = 0, \pm 1 \quad (\text{A.63})$$

are listed in Table 4.

References

- [1] K. Wilson, Phys. Rev. D 10 (1974) 2445.
- [2] G. 't Hooft, Nucl. Phys. B138 (1978) 1.
- [3] G. 't Hooft, Nucl. Phys. B153 (1979) 141.
- [4] M. Lüscher, K. Symanzik and P. Weisz, Nucl. Phys. B 173 (1980) 365.
- [5] M. Lüscher, Nucl. Phys. B 180 (1981) 317.
- [6] M. Lüscher, G. Münster and P. Weisz, Nucl. Phys. B 180 (1981) 1.
- [7] M. Lüscher and P. Weisz, JHEP 07 (2004) 014, arXiv:hep-th/0406205.
- [8] H. B. Meyer, JHEP 05 (2006) 066, arXiv:hep-th/0602281.
- [9] O. Aharony and E. Karzbrun, JHEP 06 (2009) 012, arXiv:0903.1927 [hep-th].
- [10] O. Aharony and M. Field, JHEP 01 (2011) 065, arXiv:1008.2636 [hep-th].
- [11] O. Aharony and N. Klinghoffer, JHEP 12 (2010) 058, arXiv:1008.2648 [hep-th].
- [12] O. Aharony and M. Dodelson, JHEP 02 (2012) 008, arXiv:1111.5758 [hep-th].
- [13] O. Aharony, M. Field and N. Klinghoffer, JHEP 04 (2012) 048, arXiv:1111.5757 [hep-th].

- [14] O. Aharony and Z. Komargodski, JHEP 05 (2013) 118, arXiv:1302.6257 [hep-th].
- [15] M. Billó, M. Caselle, F. Gliozzi, M. Meineri and R. Pellegrini, JHEP 05 (2012) 130, arXiv:1202.1984 [hep-th].
- [16] F. Gliozzi and M. Meineri, JHEP 08 (2012) 056, arXiv:1207.2912 [hep-th].
- [17] T. Filk, Regularization procedure for string functionals, preprint BONN-HE-81-16 (Bonn U.), Sep 1981.
- [18] K. Dietz and T. Filk, Phys. Rev. D 27 (1983) 2944.
- [19] M. Billó, M. Caselle, V. Verduci and M. Zago, PoS LATTICE2010 (2010) 273, arXiv:1012.3935 [hep-lat]
- [20] M. Billó, M. Caselle and R. Pellegrini, JHEP 01 (2012) 104, arXiv:1107.4356 [hep-th].
- [21] F. Gliozzi, M. Pepe and U.-J. Wiese, JHEP 11 (2010) 053, arXiv:1006.2252 [hep-lat].
- [22] H. B. Meyer, Phys. Rev. D 82 (2010) 106001, arXiv:hep-th/1008.1178.
- [23] B. B. Brandt, M. Meineri, arXiv:1603.06969 [hep-th].
- [24] A. Athenodorou, B. Bringoltz and M. Teper, JHEP 02 (2011) 030, arXiv:1007.4720 [hep-lat].
- [25] A. Athenodorou, B. Bringoltz and M. Teper, JHEP 05 (2011) 042, arXiv:1103.5854 [hep-lat].
- [26] A. Athenodorou and M. Teper, JHEP 06 (2013) 053, arXiv:1303.5946 [hep-lat].
- [27] A. Athenodorou and M. Teper, arXiv:1602.07634 [hep-lat].
- [28] A. Athenodorou and M. Teper, arXiv:1609.03873 [hep-lat].
- [29] G. 't Hooft, Nucl. Phys. B72 (1974) 461.
- [30] G. Veneziano, Nucl. Phys. B 117 (1976) 519.
- [31] Yu. M. Makeenko and A. A. Migdal, Nucl. Phys. B 188 (1981) 269.
- [32] A. A. Migdal, Phys. Rept. 102 (1984) 199.
- [33] O. Alvarez, Phys. Rev. D24 (1981) 440.
- [34] J. F. Arvis, Phys. Lett. B 127 (1983) 106.
- [35] J. Ambjørn and Y. Makeenko, arXiv:1601.00540 [hep-th].

- [36] Yu. Makeenko, arXiv:1206.0922 [hep-th].
- [37] Yu. M. Makeenko and P. Olesen, Phys. Rev. D 80 (2009) 026002, arXiv:0903.4114 [hep-th].
- [38] Yu. M. Makeenko, arXiv:1208.1209 [hep-th].
- [39] J. M. Maldacena, Phys. Rev. Lett. 80, 4859 (1998), hep-th/9803002.
- [40] S. J. Rey and J. T. Yee, Eur. Phys. J. C 22, 379 (2001), hep-th/9803001.
- [41] D. E. Berenstein, R. Corrado, W. Fischler and J. M. Maldacena, Phys. Rev. D 59 (1999) 105023, hep-th/9809188.
- [42] N. Drukker, D. J. Gross and H. Ooguri, Phys. Rev. D 60 (1999) 125006, hep-th/9904191.
- [43] J. K. Erickson, G. W. Semenoff and K. Zarembo, Nucl. Phys. B 582, 155 (2000), arXiv:hep-th/0003055.
- [44] L. F. Alday and J. M. Maldacena, JHEP 06 (2007) 064, arXiv:0705.0303 [hep-th].
- [45] L. F. Alday, D. Gaiotto, J. Maldacena, A. Sever and P. Vieira, JHEP 04 (2011) 088, arXiv:1006.2788 [hep-th].
- [46] D. Gaiotto, J. Maldacena, A. Sever and P. Vieira, JHEP 03 (2011) 092, arXiv:1010.5009 [hep-th].
- [47] A. V. Belitsky, G. P. Korchemsky and E. Sokatchev, Nucl. Phys. B 855 (2012) 333, arXiv:1103.3008 [hep-th].
- [48] A. Sever, P. Vieira and T. Wang, JHEP 12 (2012) 065, arXiv:1208.0841 [hep-th].
- [49] A. V. Belitsky, S. E. Derkachov and A. N. Manashov, Nucl. Phys. B 882 (2014) 303, arXiv:1401.7307 [hep-th].
- [50] A. M. Polyakov, Nucl. Phys. B 164 (1980) 171.
- [51] E. Aurell and P. Salomonson, Commun. Math. Phys. 165 (1994) 233.
- [52] M. Caselle, M. Hasenbusch and M. Panero, JHEP 03 (2005) 026, arXiv:hep-lat/0501027.
- [53] M. Caselle, M. Hasenbusch and M. Panero, JHEP 03 (2006) 084, arXiv:hep-lat/0601023.
- [54] V. Agostini, G. Carlino, M. Caselle and M. Hasenbusch, Nucl. Phys. B 484 (1997) 331, hep-lat/9607029.
- [55] H. A. Kramers and G. H. Wannier, Phys. Rev. 60 (1941) 252.

- [56] L. Onsager, Phys. Rev. 65 (1944) 117.
- [57] F. J. Wegner, J. Math. Phys. 12 (1971) 2259.
- [58] R. Balian, J. M. Drouffe and C. Itzykson, Phys. Rev. D 11 (1975) 2098 .
- [59] R. Savit, Rev. Mod. Phys. 52 (1980) 453.
- [60] M. Hasenbusch and K. Pinn, Physica A192 (1993) 342, arXiv:hep-lat/9209013.
- [61] M. Caselle, R. Fiore, F. Gliozzi and S. Vinti, Int. J. Mod. Phys. A 8 (1993) 2839, arXiv:hep-lat/920700.
- [62] M. Caselle, R. Fiore, F. Gliozzi, M. Hasenbusch, K. Pinn and S. Vinti, Nucl. Phys. B 432 (1994) 590, arXiv:hep-lat/9407002.
- [63] M. Caselle, F. Gliozzi, U. Magnea and S. Vinti, Nucl. Phys. B 460 (1996) 397, arXiv:hep-lat/9510019.
- [64] M. Caselle, R. Fiore, F. Gliozzi, M. Hasenbusch and P. Provero, Nucl. Phys. B 486 (1997) 245, arXiv:hep-lat/9609041.
- [65] Y. Deng and H. W. J. Blöte, Phys. Rev. E 68 (2003) 036125.
- [66] M. Lüscher and P. Weisz, JHEP 0109 (2001) 010, arXiv:hep-lat/0108014.
- [67] M. Lüscher and P. Weisz, JHEP 07 (2002) 049, arXiv:hep-lat/0207003.
- [68] M. Caselle, M. Hasenbusch and M. Panero, JHEP 01 (2003) 057, arXiv:hep-lat/0211012.
- [69] A. Pleijel, Arkiv för Matematik, 2 (1954) 553.
- [70] M. Kac, Amer. Math. Monthly 73 (1966) 1.
- [71] K. Stewartson and R. T. Waechter, Proc. Cambridge Phil. Soc. 69 (1971) 353.
- [72] R. Balian and C. Bloch, Ann. of Phys. 64 (1971) 271.
- [73] P. B. Gilkey, The index theorem and the heat equation (Publish or Perish, Boston, 1974).
- [74] H. P. McKean and I. M. Singer, J. Diff. Geometry 1 (1967) 43.
- [75] A. M. Polyakov, Phys. Lett. B 103 (1981) 207.
- [76] B. Durhuus, H. B. Nielsen, P. Olesen and J. L. Petersen, Nucl. Phys. B 196 (1982) 498.
- [77] B. Durhuus, P. Olesen and J. L. Petersen, Nucl. Phys. B 201 (1982) 176.

- [78] O. Alvarez, Nucl. Phys. B 216 (1983) 125.
- [79] T. A. Driscoll and L. N. Trefethen, Schwarz–Christoffel Mapping. Cambridge University Press, Cambridge, UK, 2002.
- [80] <http://www.netlib.org/conformal/>
- [81] <http://www.math.udel.edu/~driscoll/SC/index.html>